# Sex-Specific DNA Methylation and Gene Expression Changes in Mouse Placentas After Early Preimplantation Alcohol Exposure

Lisa-Marie Legault[1,2], Mélanie Breton-Larrivée[1,2], Fannie Filion-Bienvenue[1,2], Anthony Lemieux[1], Alexandra Langford-Avelar[1,2], Thomas Dupas[1,3], Serge McGraw[1,2,3,#]

[1]CHU Ste-Justine Research Center, Montréal, QC, Canada

[2]Department of Biochemistry and Molecular Medicine, Université de Montréal, QC, Canada

[3]Department of Obstetrics and Gynecology, Université de Montréal, QC, Canada

[#]Corresponding author: Serge McGraw

CHU Ste-Justine Research Center, 3175 Chemin de la Côte-Sainte-Catherine, Montréal, QC H3T 1C5, Canada

514-345-4931

serge.mcgraw@umontreal.ca

## Conflict of interest statement

The authors have declared that no conflict of interest exists.

**ABSTRACT**

The placenta is vital for proper embryonic development and successful pregnancy. Preimplantation alcohol exposure can negatively impact embryonic development and lead to fetal alcohol spectrum disorder. We and others have demonstrated the adverse effects of preimplantation alcohol exposure on embryo morphology and molecular profiles at late gestation, but studies on the placenta are markedly lacking. Here, we used an established preclinical mouse model to assess the impact of preimplantation (8-cell stage) binge-like alcohol exposure on the morphology, DNA methylation, and gene expression patterns in male and female late-gestation placentas. While overall placental morphology was not affected, we uncovered numerous differentially methylated regions (DMRs; $n$=991 in males; $n$=1309 in females) and differentially expressed genes (DEGs; $n$=1046 in males; $n$=340 in females) in the placentas. Remarkably, only 21 DMRs and 54 DEGs were common to both sexes, which were enriched for genes involved in growth factor response pathways. Using LASSO regression, we were able to precisely discriminate control and ethanol-exposed placentas based on their specific DNA methylation patterns. This is the first study demonstrating that preimplantation alcohol exposure alters the DNA methylation and transcriptomic profiles of late-gestation placentas. Importantly, it reveals a placental DNA methylation signature that can detect prenatal alcohol exposure and provide appropriate support to prevent eventual impact.

## GRAPHICAL ABSTRACT

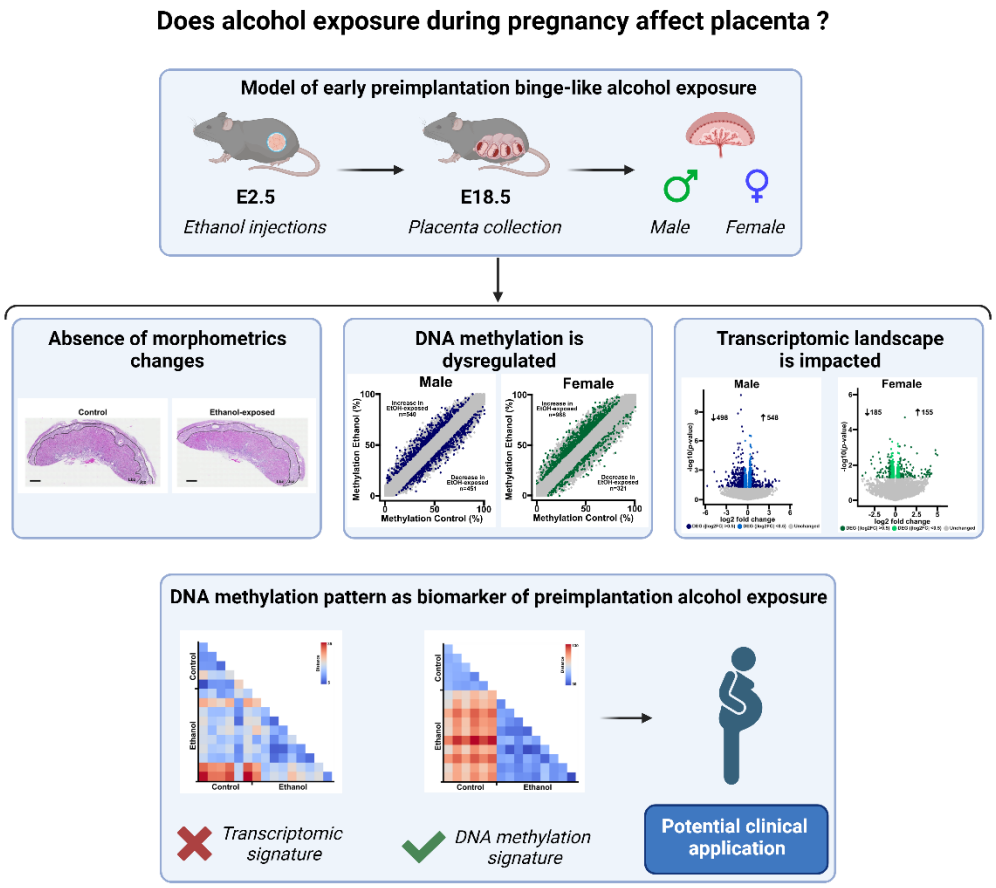

## INTRODUCTION

The placenta is a transient organ that supplies oxygen, essential nutrients, hormones, and metabolites to the developing fetus. Although commonly misconceived of as maternal, the placenta originates from the same pool of early embryonic blastomere cells that form the fetus, and shares its sex[1]. During early development, the trophectoderm and inner cell mass separate into distinct lineages, and the placenta develops alongside the embryo. In mice, placental remodeling occurs as the chorion fuses with the allantois, followed by trophoblast differentiation and labyrinth structure formation[1]. This remodeling process typically ends by mid-gestation, at E10.5 in mice and E18 in humans[1,2]. Proper placental development and function are crucial for the progression of pregnancy, and abnormalities lead to a range of adverse pregnancy outcomes, including embryonic growth delays, intrauterine growth restriction, preeclampsia, and preterm birth[3,4].

Prenatal alcohol exposure (PAE) is a leading—and preventable—cause of birth defects and neurodevelopmental issues worldwide[5]. It can cause various issues with development, cognition, and behavior, which can be lifelong. Adverse effects of alcohol exposure at any point during pregnancy are referred to as fetal alcohol spectrum disorder (FASD)[5]. FASD manifests as various symptoms, including cognitive impairments, learning difficulties, behavioral issues, and, in severe cases, profound intellectual disabilities and craniofacial abnormalities[5]. Annually, approximately 630,000 newborns are affected by FASD worldwide[6]. Its presentation and severity depend on multiple factors, including the timing, amount, and pattern of PAE[5]. Poor maternal health, exposure to other harmful substances, and nutritional deficiencies can also increase FASD severity[5]. Currently, there is no molecular diagnostic tool for FASD, and most cases are not identified until school, when neurodevelopmental symptoms become noticeable[5]. Early diagnosis and management can alleviate the impacts of FASD, while late detection often results in a need for lifelong health and social care[5].

The preimplantation period is a critical phase in embryonic development, in which the parental DNA methylation marks are erased and the epigenome is remodeled to initiate the developmental program[7]. Since pregnancy is typically detectable only after implantation, when human chorionic gonadotropin hormone production begins, there is a 6-day window of high risk for PAE during the preimplantation development stage[8]. Given the increasing rate of alcohol use, including binge drinking, among women of 18–34 years old[9], and the substantial number of unintended pregnancies worldwide (approximately 40%)[10], it is essential to investigate the impact of alcohol during this critical phase. Despite its importance for proper embryonic development and its heightened susceptibility to adverse environmental exposures, the preimplantation period has been understudied in relation to PAE, with only a few models focusing exclusively on this early developmental timepoint.

In our recent study using a preclinical mouse model of early preimplantation binge-like alcohol exposure, we reported sex-specific DNA methylation changes in the forebrains of mid-gestation (E10.5)[11]. We also observed an increased incidence of morphological defects, including growth delays, in embryos exposed to ethanol at E10.5 and E18.5[11,12]. However, a significant knowledge gap remains regarding the effects of early preimplantation alcohol exposure on the embryo and placenta.

Here, we used a mouse model of early preimplantation prenatal alcohol exposure to define its impacts on the late-gestation placenta.

## RESULTS

### Early preimplantation alcohol exposure does not induce morphometric changes in the placenta but induces lower embryo weight in males

In this study, we examined the effect of early preimplantation binge alcohol exposure on late placental development using an established FASD mouse model[11]. Briefly, to simulate short-term exposure to a

high level of alcohol, pregnant females were given two doses (2.5 g/kg) of ethanol at 2-hour intervals during preimplantation (at the 8-cell stage (E2.5)). We previously showed that this increases the average blood alcohol level to 158.31 mg/dL[11]. At late gestation (E18.5), we collected the embryos and placentas to assess the overall impacts of alcohol on gestational outcomes, focusing first on basic morphometric measurements. All measurements were compared within the same sex.

The control and ethanol-exposed groups contained 55% ($n$=47/86) and 61% ($n$=62/101) male embryos; however, this was not statistically different (Figure 1A). Additionally, there were no significant effects of early preimplantation alcohol exposure on litter size, the number of males and females per litter (Fig. 1B), or the placental area and weight (Fig. 1C-D). We observed a small but significant decrease in the weights of ethanol-exposed male embryos compared to controls (1.134 g vs 1.195 g, respectively; $p<0.01$), while no differences were observed in females (Fig. 1E). Despite the reduced weights of male embryos, placental efficiency (*i.e.*, the fetal-to-placental weight ratio) was similar between control and ethanol-exposed embryos for both sexes (Fig. 1F). We analyzed the average morphometric measurements of each litter for all four parameters and did not find any significant differences between the groups (Fig. S1).

We next assessed the impact of preimplantation alcohol exposure on global placental cell composition. After hematoxylin and eosin staining of E18.5 placental cross sections, we observed no significant differences in the areas or thicknesses of the junctional and labyrinth zones between the groups, nor in their respective area/thickness to total area/thickness ratios (Fig S2A-I). However, in females, the junctional zone thickness and the ratio of the junctional zone area to the total area significantly increased (both $p<0.05$ by $F$ test; Fig. S2).

Overall, these findings suggest that early preimplantation alcohol exposure does not significantly impact placental morphology during late gestation, but does have a developmental effect on male embryos.

**Altered DNA methylation in late-gestation placentas exposed to alcohol during preimplantation**

To examine the impact of preimplantation alcohol exposure on the DNA methylation patterns of late-gestation placentas, we performed genome-wide DNA methylation analyses. We randomly selected six control placentas (three males and three females) and 10 ethanol-exposed placentas (five males and five females) with normal morphometric measurements and no visible morphological defects. The corresponding embryos also developed normally.

After establishing sex-specific DNA methylation profiles in E18.5 placentas, we compared the average DNA methylation levels in 100 bp non-overlapping windows (tiles) between control and ethanol-exposed male or female placentas, each with a minimum of three samples per condition and a sequencing depth of at least 10×. We identified 751,083 tiles with sufficient coverage in both male and female placentas, allowing us to investigate shared and sex-specific DNA methylation differences induced by early preimplantation alcohol exposure (Fig. S3A-B).

**Sex-specific DNA methylation dysregulation in late-gestation placentas following early preimplantation alcohol exposure**

We observed a noticeable shift in the distributions of the tiles based on their DNA methylation levels in both control and ethanol-exposed placentas of males and females (Fig. S3C). Specifically, female ethanol-exposed placentas had more tiles with higher methylation levels (70–80%, 80–90%, and 90–100%) and less tiles with lower methylation levels (10–20%, 20–30%, 30–40%) than female control placentas. A similar trend was observed in male ethanol-exposed placentas, although to a lesser extent. Strikingly, we identified 991 and 1309 differentially methylated regions (DMRs) in response to early preimplantation alcohol exposure that were exclusive to males and females, respectively, while only 21 DMRs were shared between the sexes (Fig. 2A and C; Fig. S3A; Table 1). Male placentas had nearly equal distributions of DMRs, displaying both increased ($n$=540, 54%) and decreased ($n$=451, 46%)

methylation after ethanol exposure (Fig. 2A). In contrast, DMRs in female placentas were predominantly increased (*n*=988 (75%) vs. *n*=321 (25%); Fig. 2C). Most DMRs were annotated as in introns (male, 41%; female, 42%) or intergenic regions (male, 39%; female, 37%; Fig. 2B and D). We observed greater methylation changes between control and ethanol-exposed placentas in DMRs located in non-coding regions (average methylation in controls, 44%; ethanol-exposed, 51%) and in exons (average methylation in controls 47%; ethanol-exposed 52%) in males, while in females, greater changes were observed for DMRs located in 3′ UTRs (average methylation in controls, 53%; ethanol-exposed, 63%) and introns (average methylation in controls, 45%; ethanol-exposed, 54%; Fig 2B and D).

The distributions of sex-specific DMRs across different CpG methylation levels followed a consistent trend between the sexes. Regions with higher methylation levels tended to gain methylation following ethanol exposure, while regions with lower methylation levels tended to lose methylation (Fig. 2E and G). This trend was particularly pronounced for female-specific DMRs, with significant differences in the distributions of the 1309 tiles across nearly all methylation categories (Fig. 2G). Most sex-specific DMRs exhibited modest methylation changes (10–15%). In terms of magnitude, more female-specific DMRs (12%) exhibited methylation changes > 20% than male-specific DMRs (9%; Fig. 2F and H). However, very few DMRs changed by > 30%: only ~1% (*n*=15) and 0.4% (*n*=4) of female- and male-specific DMRs, respectively.

To identify pathways associated with sex-specific DMRs in ethanol-exposed placentas, we performed gene annotation enrichment analyses in Metascape. After removing tiles from intergenic regions, the remaining male DMRs occurred in 607 regions representing 542 unique genes. Enriched pathways included cell junction assembly (*Cttn*, *Mapt*), response to growth factors (*Fgf1*, *Zeb2*), negative regulation of synaptic transmission (*Cttn*, *Mapt*), organic hydroxy compound biosynthesis, (*Slc11a2*, *Star*), and phenol-containing compound biosynthesis (*Hdc*, *Nr4a2*) (Fig. 2I-2J). Remaining female-specific DMRs occurred in 821 regions corresponding to 749 unique genes. The top enriched pathways

differed from in males, including plasma membrane-bounded cell projection morphogenesis (*Ank3*, *Cdh11*), regulation of inflammatory responses (*Bcl6*, *Foxj1*), alpha-beta T cell differentiation (*Bcl6*, *Foxj1*), negative regulation of cell migration (*Rbp4*), and negative regulation of cell population proliferation (*Foxj1*, *Wnt5a*) (Fig. 2I-J).

These findings reveal that early preimplantation alcohol exposure results in sex-specific DNA methylation dysregulation in late-gestation placentas, with females showing a higher susceptibility. Furthermore, these sex-specific alterations in DNA methylation are associated with specific biological pathways.

**Female ethanol-exposed placentas tend to lose methylation in CpG-rich regions**

To determine if the local genomic sequence contributes to the intrinsic sex-specific susceptibility of DMRs, we analyzed their CpG contexts using publicly available CpG island tracks. We categorized DMRs into CpG islands, CpG shores (±2 kb from CpG islands), CpG shelves (±2 kb from CpG shores), or open sea (>2 kb from CpG shelves). Most male and female DMRs were in open sea regions with low CpG content (Fig. S4A). We found that the highest proportions of DMRs located in CpG islands (CpG-rich regions) had increased methylation in males (13%; $n$=68) and decreased methylation in females (14%; $n$=45). In female placentas, DMRs with decreased methylation present at the highest proportion in CpG shores (28%; $n$=89), with other groups having similar proportions (16–18%) (Fig. S4A). The largest changes in methylation levels occurred in open sea regions and shores, and the smallest changes mainly occurred in CpG islands (Fig. S4B).

To more broadly evaluate the methylation differences of sex-specific DMRs based on their CpG contexts, we compared the methylation profiles of DMRs in CpG islands (high CpG content), promoters (mid CpG content), and repeat regions (low CpG content; Fig. S4C). Generally, male DMRs in CpG islands had higher methylation in ethanol-exposed placentas than in controls. This difference lessened

with decreasing CpG density, consistent with the fact that DMRs in repeat regions displayed both decreased and increased methylation levels in ethanol-exposed placentas compared to controls. Interestingly, we observed the opposite trend when examining the methylation profiles of female DMRs across different annotations. While we observed generally lower methylation levels for DMRs in CpG islands in ethanol-exposed placentas, the methylation levels of DMRs in promoters and particularly in repeat regions increased in female ethanol-exposed placentas compared to controls (Fig. S4C; bottom panels). Taken together, our findings suggest that early preimplantation alcohol exposure differentially impacts the placental epigenome depending on sex and CpG density.

**DMRs shared by male and female late-gestation placentas after early preimplantation alcohol exposure are related to growth and development**

Although our primary focus was to identify sex-specific DMRs in the placenta resulting from early preimplantation alcohol exposure, we also observed shared affected regions between sexes. Of the 21 shared DMRs (Table 2), most (16) exhibited methylation differences of < 15% between ethanol-exposed and control placentas, with the largest difference being 23% (Fig. 3A). Regions of interest included DMRs located in genes such as *Galp* (neuropeptide signaling), *Psd3* (protein transduction), or *Wwox* (apoptotic signaling; Fig. 3B). Most (17) shared DMRs increased or decreased consistently in both sexes, while four displayed opposing changes (Fig. 3A). Twelve DMRs were in promoters or intragenic regions. Pathway enrichment analysis revealed enrichment in growth pathway regulators (Fig. 3C-D).

For a broader understanding of how preimplantation alcohol exposure alters the DNA methylation patterns of specific genes in both male and female placentas, we performed DMR comparisons based on gene annotations instead of genomic positions. After excluding intergenic DMRs, we compared a total of 607 male-specific DMRs ($n$=542 genes) to 821 female-specific DMRs ($n$=749 genes) located in promoters and intragenic regions. Along with the 21 shared DMRs previously described, we uncovered 69 shared genes across 89 DMRs with DNA methylation differences in male or female ethanol-exposed

placentas (Fig. S5A). These included methylation changes that were consistent ($n$=39) and opposing ($n$=50) between the sexes (Fig. S5A-B). Pathway enrichment analysis revealed pathways related to the reproductive process, cell morphogenesis, transmembrane transport activity, myeloid cell development, and response to growth factors, with regions associated with *Bmp6*, *Prdm14*, *Ptprk*, and *Runx1* affected (Fig. S5C-D).

These findings indicate that the dysregulated pathways shared between male and female placentas in response to preimplantation alcohol exposure likely contribute to the adverse effects observed in male and female embryonic development earlier in development (E10.5) as previously published using this model[11].

**Early preimplantation alcohol exposure leads to sex-specific gene expression changes in late-gestation placentas**

To further our understanding of the molecular impact of preimplantation alcohol exposure on the late-gestation placenta, we performed gene expression profiling *via* mRNA-Seq. We used a significance threshold of $p<0.05$ to identify differentially expressed genes (DEGs) between ethanol-exposed and control placentas. Of 31,235 expressed genes, we identified 1046 male-specific DEGs, 340 female-specific DEGs, and 54 shared DEGs (Fig. 4A-D; Fig. S6A-B; Table 3). In males, 498 genes showed decreased expression in ethanol-exposed placentas, while 548 genes showed increased expression (Fig. 4A and C). Although females had more DMRs than males, DEGs did not follow the same trend. Of the 340 female-specific DEGs in ethanol-exposed placentas, 185 and 155 showed decreased and increased expression, respectively (Fig. 4B and D).

Functional enrichment analyses of male- and female-specific DEGs revealed divergent pathways. For instance, male DEGs were related to cell migration (*Aqp1*, *Rhoc*), cytoskeletal organization (*Apoa1*, *Bmp10*), cell-substrate adhesion (*Adam8*, *Utrn*), cell junction organization (*Ank6*, *Cdh6*), and blood

vessel development (*Flt4*, *Slc16a1*) (Fig. 4E); whereas the female DEGs showed enrichment in pathways involved in cell adhesion (*Itgb3*, *Ret*), serotonin uptake (*Slc22a2*, *Snca*), PIWI-interacting RNA metabolism (*Fkbp6*, *Piwil2*), megakaryocyte development and platelet production (*Gata2*, *Gata4*), and locomotory behavior (*Chrna4*, *Efnb3*) (Fig. 4F). Examples of male- and female-specific DEGs are shown in Figure 4G-H.

**Shared gene expression changes in late-gestation placentas after early preimplantation alcohol exposure**

We also identified 54 genes (Table 4) that showed similar differential expression in both male and female ethanol-exposed placentas following early preimplantation alcohol exposure. For most genes (50), we observed comparable changes in normalized read counts and fold changes between the sexes (Fig. S7A-C); however, four genes showed divergent changes in males and females, including *Ifit2* (response to interferon-alpha) and *Krt14* (cytoskeleton organization; Fig. S7D). For *Ifit2*, the control expression level also differed between males and females (Fig. S7D).

Pathway enrichment analysis of these shared DEGs revealed enrichment in several pathways, including neuromuscular junction development (*Musk*, *Pmp22*), sphingolipid biosynthesis (*B3gnt5*, *St8sia5*), artery development (*Chd7*, *Luzp1*), and matrix organization (*Foxf2*, *Kif9*) (Fig. S7E). Additional interesting shared DEGs included *Bhlhe41* (associated with muscle development) and *Cited2* (involved in decidualization, placenta, cardiac, and cortex development), which both showed decreased expression in ethanol-exposed placentas, and *Scel* (which regulates Wnt signaling) and *Syt14* (involved in synaptic transmission), which exhibited increased expression (Fig. S7F). These specific DEGs highlight potential molecular mechanisms and pathways affected by preimplantation alcohol exposure in the placenta regardless of sex. These findings provide insights into the biological processes that may be impacted by preimplantation alcohol exposure in both male and female placentas, suggesting potential negative consequences of placental dysfunction on embryonic development following early PAE[11].

**Early preimplantation alcohol exposure does not strictly impact genes crucial for placental development or placental imprinting genes at late gestation**

To evaluate the impact of early preimplantation alcohol exposure on genes crucial for placental development, we analyzed our DNA methylation and gene expression datasets using previously published curated gene lists [13].

Of the 205 curated placental genes , 193 were present in our DNA methylation dataset, accounting for 7327 tiles located in promoters and intragenic regions (Fig. S8A). However, only six contained DMRs: three in males (*Epas1*, *Id1*, and *Peg10*) and three in females (*Flt1*, *Ppard*, and *Serpine1*). All 205 curated placental genes were included in our mRNA-Seq dataset, of which 19 and eight were dysregulated following ethanol exposure in males and females, respectively (Fig. S8B). Only one DEG, *Cited2*, was changed in both male and female placentas (Fig. S7B, C, and F and Fig. S8B). Additionally, *Peg10*'s intronic DMR, which overlaps with the gene's imprinting control region (ICR), exhibited increased DNA methylation and increased expression in ethanol-exposed placentas (Fig. S8A).

To further investigate the impact of preimplantation alcohol exposure on imprinted genes, we searched our datasets for a curated list of 105 genes known to be regulated by genomic imprinting in the placenta [14-19]. In male ethanol-exposed placentas, we identified 17 DMRs located in the promoters or intragenic regions of 11 genes (Fig. S9A and C; Table S1). Of these, 12 DMRs in seven genes were located in the ICR. Furthermore, we observed 18 imprinted DEGs in male placentas (Fig. S8B; Table S1). In contrast, female ethanol-exposed placentas showed fewer DNA methylation changes on imprinting genes, with only nine DMRs in nine different genes. Of these, only *Slc22a2* showed differential expression (Fig. S9A-B; Table S1). Detailed examples of DMRs (*Airn*, *Commd1*, *Grb10* and *Peg10*) and DEGs (*Grb10*, *Igf2r*, *Peg10*, *Zrsr1* and *Slc22a2*) for male and female placentas are shown in Figure S9C-D.

These results reveal that although several placental and imprinted genes exhibited dysregulated DNA methylation levels or expression following early preimplantation alcohol exposure, the dysregulation was not widespread. These findings align with our morphometric analyses, which did not reveal any significant placental malformations or dysfunctions.

**Sex-specific regions with both DNA methylation and gene expression changes in the late-gestation following early preimplantation alcohol exposure**

To explore the relationship between dysregulated DNA methylation and gene expression profiles in the placenta after preimplantation alcohol exposure, we next compared our lists of intragenic DMRs and DEGs by examining the expression profiles of the genes associated with 607 male DMRs (542 unique genes), 821 female DMRs (749 unique genes), and 12 shared DMRs (11 unique genes).

Of the 11 genes with shared DMRs, only *Clstn3* and *Tro* exhibited gene expression changes in male ethanol-exposed placentas (Fig. S10A-B), and no expression changes were observed in females. In males, 40 unique genes containing 46 DMRs displayed both DNA methylation and gene expression changes in ethanol-exposed placentas (Fig. 5A). The majority of these DMRs (78%; $n$=36) exhibited 10–20% changes in DNA methylation and resulted in small expression changes (|log2FC| < 0.5; Fig. S11A). Notably, regions/genes with altered methylation and expression included *Apoc1* (lipid activity), *Carmil1* (implicated in actin filament processes), *Slc16a3* (encodes the MCT4 protein, important for transmembrane transport, placental organization, and vascularization) and *Zfhx3* (a transcription factor important for development; Fig. 5B).

In females, 15 unique genes containing 16 DMRs showed both differential methylation and gene expression changes in ethanol-exposed placentas (Fig. 5C). In contrast to males, 11 of these DMRs (69%) showed > 20% changes in methylation, and seven genes (47%) changed expression by |log2FC| > 0.5 in ethanol-exposed placentas (Fig. S11B). Noteworthy genes included *Chd7* (implicated in cardiac, muscle,

and neuronal development), *Cux2* (related to neuronal pathways and functions, including cortical interneuron development), *Elovl2* (involved in fatty acid processes), and *Mfsd2a* (implicated in the establishment of the blood-brain barrier; Fig. 5D).

These results provide valuable insights into the long-term impacts of preimplantation alcohol exposure on several genes and emphasize the significance of sex-specific DNA methylation dysregulation in shaping the gene expression patterns of male and female placentas.

**Dysregulated placental DNA methylation as a biomarker for early preimplantation alcohol exposure**

To address the lack of a detection method for PAE and FASD shortly after birth, we explored the potential of using specific molecular patterns present in ethanol-exposed placentas. We used a random forest classifier and least absolute shrinkage and selection operator (LASSO) regression, a machine-learning technique, to create a diagnostic model using identifiable markers found in our transcriptomic or DNA methylation data. To enhance accuracy and effectiveness, we trained the model using both male and female samples together, increasing our statistical strength and refining the analytical process.

First, we used gene expression profiles and performed LASSO regression to establish specific transcriptomic signatures for ethanol-exposed placentas. Despite being statistically significant, the 20 DEGs identified were not different enough between the conditions to establish a good transcriptomic signature of preimplantation alcohol exposure in late-gestation placentas, with small Euclidean distances between samples of the two conditions and poor statistical coefficient of importance (Fig. S12A-C).

However, LASSO regression using our DNA methylation profiles identified a set of 24 statistically significant DMRs that formed a specific signature enabling the effective discrimination of ethanol-exposed samples from controls for both principal component analysis and Euclidean distance calculations (Fig. 6A-B). These DMRs were both intragenic ($n$=15) and intergenic ($n$=9), and each had

different levels of importance based on their statistical parameters, notably the LASSO coefficient, Wilcoxon *p*-value, and AUC generated by LASSO analysis (Fig. 6C). The most significant DMR in the signature was located in an intergenic region close to *Nup35*. Additionally, there were DMRs in genes such as *B3galt1*, *Kcng1*, *Mir3960*, *Mir6940*, *Psd3*, and *Sesn1*, along with intergenic DMRs close to *Bicd1*, *Gatsl2*, and *Zeb2* (Fig. 6C-D). These results reveal a specific DNA methylation pattern in the placenta that can be used as a dependable molecular tool for detecting early embryonic PAE at birth.

## DISCUSSION

In this study, we examined the molecular and developmental effects of PAE during early preimplantation on the late-gestation placenta. Our analyses are the first to reveal extensive sex-specific alterations in DNA methylation and gene expression patterns in late-gestation mouse placentas exposed to ethanol. Interestingly, despite these molecular changes, the overall morphological development of the placenta appeared unaffected. Through machine learning, we successfully identified a DNA methylation signature for identifying offspring exposed to alcohol during the early embryonic stages.

### Sex-specific impacts of preimplantation alcohol exposure on fetal growth and related pathways

Prenatal alcohol exposure was previously shown to alter embryonic development in different contexts, by inducing fetal growth restriction or growth delay[11,12]. With our model, we found that the impact on growth and related pathways was more pronounced in male ethanol-exposed placentas, consistent with the observed male-specific changes in genes regulating growth, cytoskeletal organization, placental development, and vascularization. Furthermore, we noted a reduction in fetal weight only in male embryos, indicating that males may be more susceptible to growth delays following preimplantation alcohol exposure. However, it is worth noting that in our previous studies using this model, we observed similar percentages of growth-delayed embryos (~5%) between males and females at mid-gestation[11]. It

is possible that some female embryos with growth delays at mid-gestation may catch up later in development, eventually achieving a similar fetal weight to control embryos. Several studies have demonstrated that female embryos generally exhibit greater adaptability to adverse *in utero* environments than male embryos, facilitating their development even in the presence of altered resource availability[20-22]. Male ethanol-exposed placentas displayed altered methylation and/or expression patterns in several genes that are directly linked to embryonic growth restriction. For example, a study recently showed injecting *Fgf2* (downregulated) into a rat model of preeclampsia improved clinical outcomes, including attenuating fetal growth restriction[23]. Mutation of *Fgf1* (increased methylation) has been linked to preeclampsia in humans[24], while *Bmp6* (decreased methylation) was downregulated in the fetal kidneys of rats with intrauterine growth restriction in a model of induced hypertension due to chronic insulin administration[25]. Changes in these genes may significantly contribute to the inability of male embryos to develop normally and achieve the fetal weights of control embryos.

**Preimplantation alcohol exposure had a greater impact on imprinted and placental development genes in male placentas**

The methylation patterns of the ICRs of imprinted genes and the DNA methylation and expression patterns of genes crucial for placental development can significantly influence proper embryo development[26,27]. While placental development being largely completed by late gestation, epigenetic and transcriptomic dysregulation of key genes can disrupt its function, especially when the dysregulation occurs at earlier developmental stages[28]. Although histological analysis of the junctional and labyrinth zones showed comparable results between ethanol-exposed and control placentas in both sexes, we observed more changes in imprinted and placental development genes in male ethanol-exposed placentas compared to females.

Among the dysregulated genes, we observed differential methylation and expression of the imprinted gene *Grb10* in male ethanol-exposed placentas. *Grb10* encodes a growth restrictor, and

irregular imprinting, especially in its ICR, can directly affect embryonic development[26]. The increased *Grb10* expression observed in male ethanol-exposed placentas could therefore directly impact embryonic growth and development. Additionally, we observed dysregulation in both DNA methylation and gene expression in the *H19*/*Igf2* cluster, including increased expression of *Igf2r* in male ethanol-exposed placentas and increased methylation in the ICR of *Airn* (antisense of *Igf2r*). Like *Grb10*, *Igf2r* negatively regulates embryonic growth and development[26,29]. This imprinted cluster has been previously identified using a similar paradigm of alcohol exposure during preimplantation. In their study, Haycock and Ramsay showed decreased DNA methylation in the ICR of *H19* in the mid-gestation[30]. They also observed significant decreases in the weights of both ethanol-exposed fetuses and placentas at mid-gestation and found a strong correlation between DNA methylation of the paternal *H19* allele and weight loss in the ethanol-exposed group[30]. The abnormal methylation and expression profiles of imprinted genes collectively impact proper embryonic development, contributing to the observed reduced fetal weight in alcohol-exposed males.

Analysis of placental development genes also revealed more genes with altered expression profiles in male ethanol-exposed placentas. Notably, we observed increased expression of *Dnmt3l*, a coactivator of *Dnmt3a* and *Dnmt3b*, which catalyze *de novo* DNA methylation[31]. During placental development, *Dnmt3l* is essential for establishing proper maternal gene imprinting profiles and is highly expressed in trophoblasts[31-33]. While the impact of *Dnmt3l* overexpression on the placenta is unknown, studies have demonstrated morphological defects and abnormal trophoblast patterns in *Dnmt3l* knockout mice, providing further evidence of its critical role in proper embryonic development[34,35]. We cannot exclude the potential impact of dysregulated *Dnmt3l* expression on the irregular DNA methylation and transcriptomic profiles observed in certain imprinted genes, such as the maternally methylated genes *Peg10*, *Jade1*, or *Zrsr1*, in male ethanol-exposed placentas.

**Dysregulation of the placental epigenetic and transcriptomic landscape could play a role in proper embryonic brain development**

The placenta-brain axis has recently received considerable attention, and it is now well-established that placental dysregulation can lead to adverse effects on brain development and function[22,36]. Neurodevelopmental disorders and intellectual disabilities are commonly observed in FASD, resulting from disruptions during brain development and incomplete maturation[5]. While the impact of endocrine placental dysfunction on brain development is increasingly understood, the role of placental epigenetic and transcriptomic dysregulation has been less explored. Among the many enriched pathways observed in our datasets, two main pathways emerged that could directly affect normal embryonic brain development.

First, we found that male-specific DMRs were enriched for components of a pathway related to synaptic transmission, with dysregulated genes including *Asic1*, *Cbln1*, and *Plk2*. *Asic1* and *Cbln1* are required for normal neuronal development[37,38], and *Plk2* has been linked to epilepsy because of its role in synaptic potentiation[39]. Additionally, our transcriptome analysis revealed that one of the main pathways enriched in female ethanol-exposed placentas was related to serotonin metabolism. Serotonin is a neurotransmitter that regulates embryonic neurodevelopment, and the placenta plays a neuroendocrine role by producing and providing serotonin to the developing forebrain[40]. Placental insufficiency, including failing to provide an adequate serotonin supply to the embryo, is associated with the development of mental health issues and reduced cognitive abilities[40]. Knockout of *Itgb3*, which was downregulated in female ethanol-exposed placentas, had adverse effects on the placenta's vascularization structure in a sheep model, compromising nutrient transport[41]. ITGB3 is also directly involved in serotonin uptake by interacting with different serotonin transporters[42]. *Slc22a2* was overexpressed in female ethanol-exposed placentas. In addition to being imprinting in the placenta, this gene has been implicated in serotonin clearance[43]. Together, changes in these two genes could negatively modulate

serotonin uptake in the developing brain *via* altered placental endocrine function and disrupted communication, further emphasizing the impact of the placenta on embryonic health and development.

**Distinct patterns of DNA methylation dysregulation in female and male ethanol-exposed placentas**

DNA methylation analysis of late-gestation placentas following preimplantation alcohol exposure uncovered sex-specific DMRs. Moreover, we also observed sex-specific alteration patterns. While male ethanol-exposed placentas had similar numbers of increased and decreased DMRs, female ethanol-exposed placentas displayed a higher proportion of increased DMRs. Interestingly, we observed that almost half of the decreased DMRs in the female ethanol-exposed placentas were located in CpG islands, shores, or shelves, the vast majority of female DMRs with increased methylation were located in open sea regions. Conversely, most male DMRs were located in open sea regions, regardless of the direction of the change. This suggests a sex-specific effect on DNA methylation based on CpG content following preimplantation alcohol exposure.

In a recent study, we discovered genome regions with sex-biaised DNA methylation profiles in control placentas at E18.5[13]. When we compared the DMRs observed following preimplantation alcohol exposure with these sex-biased regions, we found that 115 male DMRs and 188 female DMRs were also sex-biased at late gestation. Importantly, these ethanol-exposed DMRs and sex-biased regions exhibited distinct CpG distributions based on sex. Notably, we observed a higher proportion of female-specific DMRs located in sex-biased regions in CpG islands and shores than male-specific DMRs located in sex-biased regions[13]. These differentially methylated regions between male and female embryos could help explain the sex-specific changes observed in both DNA methylation and gene expression. It is known that sex-biased differences exist during early development, and that divergent DNA methylation profiles can contribute to sex-specific DMRs in late-gestation placentas. One hypothesis is that these specific regions are more vulnerable to harmful exposures from the maternal environment due to their sex-specificity during development. Epigenetic dysregulation in these specific regions may progress

differently in males and females, resulting in sex-specific DMRs in the late-gestation following preimplantation alcohol exposure.

Further studies investigating dysregulated DNA methylation in the trophectoderm and placenta during early development could provide insights into the variability of these sex-specific regions after preimplantation PAE. Understanding the dynamics and mechanisms underlying these sex-specific effects will contribute to our knowledge of how PAE impacts placental function and subsequent developmental outcomes in a sex-dependent manner.

**Dysregulated placental DNA methylation as a biomarker for early preimplantation alcohol exposure**

Finding a molecular diagnostic tool for early detection of FASD would be an unprecedented advance in the treatment and care of affected neonates. In recent years, two different Canadian research groups showed DNA methylation changes in buccal epithelial cell swabs from children with confirmed FASD[44-46]. Moreover, one of these studies applied a machine learning approach with the identified epigenetic signature to train and further efficiently validate the identification of confirmed FASD cases [46]. Although these cells are easily accessible and require no invasive procedure to obtain, their epigenome will vary with age and may generate some bias in the generation of accurate DNA methylation signatures. Moreover, the high renewal rate of these surface cells may not homogeneously reveal PAE-induced epigenetic modifications. PAE's heterogenous paradigms and their effects on the epigenomes of buccal epithelial cells are also an obstacle in establishing a universal DNA methylation signature. Tissues or cell types more directly exposed to alcohol during gestation may be more promising alternatives. In this perspective, the placenta could be an effective means to detect FASD at birth, since its development occurs rapidly during gestation. A previous study using preconception and gestational cannabis also observed shared changes in DNA methylation in the placentas and brains of exposed embryos[47], indicating that the placenta may be able to effectively mirror some epigenetic alterations present in the

brain. Our study showed that even if alcohol exposure happens as early as the 8-cell stage, lasting DNA methylation changes occur in the placenta. Furthermore, we were able to establish a unique signature to distinguish control and ethanol-exposed samples using machine learning. The short lifespan of the placenta (resulting in minimal cell renewal) makes it an optimal candidate tissue to profile epigenetic alterations caused by PAE any time during gestation. The placenta can be thought of as an organ having a high potential to teach us more about what transpired during pregnancy and how it may have affected embryonic development. By identifying epigenetic signatures for various PAE paradigms and patterns in the placenta at birth, we could establish a reliable diagnostic tool to enable optimal support for newborns with FASD from their early life.

## CONCLUSION

In this study, we showed that early preimplantation alcohol exposure can alter the molecular profile of late-gestation mouse placentas. More precisely, our study provides valuable insights into the sex-specific epigenetic and transcriptomic consequences of early PAE on the placenta, contributing to a better understanding of its potential effects on placental function and fetal development. Furthermore, this study highlights for the first time that the placental DNA methylation profile could be an excellent molecular diagnostic tool for early PAE detection. Further studies based on our model will help decipher the mechanisms of sex-specific placental DNA methylation and gene expression changes on embryonic development and their long-term implications.

## METHODS

### Mouse model of preimplantation alcohol exposure

Eight-week-old female and male C57BL/6 mice (Charles River Laboratories) were mated, and pregnancy with E0.5 embryos was confirmed by the presence of a visible copulatory plug the following morning. Pregnant females were separated from the males and housed together ($n$=2–3) in a 12-h light/dark cycle with unrestricted access to food and water. Like in our previously published preimplantation binge-like PAE model[11], pregnant females were injected with two doses of either 2.5 g/kg 50% ethanol or an equivalent volume of saline at 2-h intervals on E2.5 (the 8-cell stage), then housed under similar conditions with limited handling during gestation.

### Tissue collection and analysis

At E18.5, pregnant females were euthanized and embryos and placentas were collected. The maternal tissue layer was then removed from the placenta. The embryos and placentas were weighed, and the placental area was calculated using a Leica stereo microscope and Leica LasX software. Placentas were flash frozen in liquid nitrogen and stored at -80°C for subsequent DNA and RNA extraction. The sex of each embryo and its placenta was determined by analyzing digested embryonic tail DNA by qPCR (LightCycler 96, Roche) for *Ddx3x* and *Ddx3y*[11,12].

### Histological analysis

On E18.5, placentas with the maternal decidua to facilitate handling. Placentas were fixed in 4% paraformaldehyde, post-fixed in 70% ethanol for 48 h, and then divided into two identical sections for paraffin embedding. Cross-sections (5 µm thick) were stained with hematoxylin and eosin and imaged on a Zeiss Zen Axioscan Slide Scanner. Image processing and junctional and labyrinth zone measurements were performed with ImageJ.

**DNA/RNA extraction and library preparation**

Six control placentas (one male and female per litter from three different litters) and 10 ethanol-exposed placentas (one male and female per litter from five different litters) were randomly selected. Whole placentas were ground in liquid nitrogen and equivalent amounts of each sample were used for DNA and RNA extraction using QIAamp DNA Micro (Qiagen #56304) and RNeasy Mini (Qiagen #74004) kits, respectively, following the manufacturer's recommendations. DNA and RNA were quantified on a QuBit Fluorimeter using Broad-Range DNA assay (ThermoFisher #Q32853) and High Sensitivity RNA assay (ThermoFisher #Q32852) kits, respectively.

DNA (1 µg) was used to produce Methyl-Seq libraries using a SureSelectXT Methyl-Seq Target Enrichment System with a mouse enrichment panel (Agilent #G9651B and #5191-6704) following the manufacturer's recommendations. After final amplification/indexation, libraries were quantified using a QuBit fluorimeter with a High Sensitivity DNA assay kit (ThermoFisher #Q32854) and quality was assessed using a BioAnalyzer before paired-end sequencing on a NovaSeq6000 S4 at the Genome Quebec core facility. We obtained 112–139 M reads per sequenced library.

High-quality RNA (500 ng) was used to produce mRNA-Seq libraries using NEBNext mRNA stranded library kits at the Genome Quebec core facility, followed by paired-end sequencing on a NovaSeq6000 S4. We obtained 26–43 M reads per sequenced library.

**Bioinformatics analysis**

Methyl-Seq results were analyzed using the GenPipes Methyl-Seq pipeline (v3.3.0)[48]. Reads were aligned to the mouse reference genome (mm10) and methylation calls were obtained with Bismark (v0.18.1)[49]. The R package MethylKit (version 1.8.1)[50] was used to obtain DMRs based on the Benjamini–Hochberg false discovery rate procedure. We used fixed parameters, such as 100-bp stepwise tiling windows and a threshold of $q < 0.01$. DNA methylation levels were calculated as the average

methylation of all CpGs within a tile for all the samples within a condition (minimum 3 samples/condition/sex at ≥ 10× sequencing depth)[11,51]. The bisulfite conversion rate (> 96%) and number of CpGs per tile were obtained using a custom Perl script[11].

Annotation of all analyzed tiles was conducted using Homer (version 4.10.1) with the mouse mm10 reference genome[52]. Functional enrichment analyses were performed with Metascape[53] using differentially methylated tiles located in genes as an input. We obtained CpG island coordinates of the mm10 genome from the UCSC Genome Browser[54], then delineated CpG shores and shelves by extending 0–2 and 2–4 kb from them, respectively, as described previously[11,51]. Statistical analyses were performed using R (version 3.5.0) or GraphPad Prism (version 9.5.0).

For mRNA-Seq data, post-sequencing bioinformatics analyses were performed on the mouse reference genome (mm10) using the GenPipes RNA-Seq pipeline (v4.1.2)[48], including tools such as Trimmomatic (v0.36)[55], STAR (v2.5.3)[56], Picard (v2.9.0), and BWA (v0.7.12)[57]. DEGs were obtained using the R package DESeq2 (v1.24.0) [58]. Genes with $p$-values < 0.05 were considered significant.

To establish a molecular signature of early preimplantation PAE, we used L1-regularized linear regression (LASSO)[59,60] with cross-validation for the gene expression and DNA methylation profiles. The curse of dimensionality (*i.e.*, challenges stemming from training models on datasets with a large number of features relative to samples) was addressed using the Synthetic Minority Over-sampling Technique to counteract sample imbalances[61]. A random forest classifier was trained on these balanced datasets to emphasize the significance of the selected DEGs and DMRs in the classification. The specific regions used to establish the signature were among the top ranked based on feature importance. The efficacy of the identified biomarkers to differentiate the two groups was validated by two-sample $t$-test and Wilcoxon rank-sum test, while ROC curves were used to assess the discriminatory capacity of each biomarker[60].

### Statistics

Statistical analyses not included in bioinformatic pipelines were performed using R (version 3.5.0) or GraphPad Prism (version 9.5.0). Statistical significance was calculated using unpaired *t*-tests with Welch's correction and an *F* test for variance. All data represent the mean ± standard deviation (SD). *P*-values $< 0.05$ were considered significant.

### Study approval

All animal work conducted in this study was approved by the CHU Ste-Justine Research Center *Comité Institutionnel de Bonnes Pratiques Animales en Recherche* (CIBPAR) under the guidance of the Canadian Council on Animal Care (CCAC).

### Data availability

All sequencing datasets generated and used in this study will be publicly available via the Gene Expression Omnibus.

## AUTHOR CONTRIBUTIONS

LML and SM designed the study. LML and MBL conducted experiments and contributed to data acquisition. LML, ALA, AL, and FFB participated in data analysis. LML, TD, and SM wrote the manuscript. All authors read and approved the final manuscript.

**ACKNOWLEDGEMENTS**

We thank the McGraw lab for their critical comments and suggestions, Karine Doiron and Elizabeth Maurice-Elder for editing, the staff of the Centre de Recherche du CHU Sainte-Justine animal facility for their assistance and the Centre d'expertise et de services Génome Québec.

## REFERENCES


1. Hemberger M, Hanna CW, Dean W. Mechanisms of early placental development in mouse and humans. *Nature reviews Genetics.* 2020;21(1):27-43.
2. Simmons DG, Natale DR, Begay V, Hughes M, Leutz A, Cross JC. Early patterning of the chorion leads to the trilaminar trophoblast cell structure in the placental labyrinth. *Development (Cambridge, England).* 2008;135(12):2083-2091.
3. Wadhwa PD, Entringer S, Buss C, Lu MC. The contribution of maternal stress to preterm birth: issues and considerations. *Clinics in perinatology.* 2011;38(3):351-384.
4. Coussons-Read ME. Effects of prenatal stress on pregnancy and human development: mechanisms and pathways. *Obstetric medicine.* 2013;6(2):52-57.
5. Popova S, Charness ME, Burd L, et al. Fetal alcohol spectrum disorders. *Nature reviews Disease primers.* 2023;9(1):11.
6. Lange S, Probst C, Gmel G, Rehm J, Burd L, Popova S. Global Prevalence of Fetal Alcohol Spectrum Disorder Among Children and Youth: A Systematic Review and Meta-analysis. *JAMA pediatrics.* 2017;171(10):948-956.
7. Canovas S, Ross PJ. Epigenetics in preimplantation mammalian development. *Theriogenology.* 2016;86(1):69-79.
8. Cole LA. New discoveries on the biology and detection of human chorionic gonadotropin. *Reproductive biology and endocrinology : RB&E.* 2009;7:8.
9. Organization WH. *Global status report on alcohol and health 2018.* World Health Organization; 2019.
10. Sedgh G, Singh S, Hussain R. Intended and unintended pregnancies worldwide in 2012 and recent trends. *Studies in family planning.* 2014;45(3):301-314.
11. Legault LM, Doiron K, Breton-Larrivée M, et al. Pre-implantation alcohol exposure induces lasting sex-specific DNA methylation programming errors in the developing forebrain. *Clinical epigenetics.* 2021;13(1):164.
12. Breton-Larrivée M, Elder E, Legault LM, Langford-Avelar A, MacFarlane AJ, McGraw S. Mitigating the detrimental developmental impact of early fetal alcohol exposure using a maternal methyl donor-enriched diet. *FASEB journal : official publication of the Federation of American Societies for Experimental Biology.* 2023;37(4):e22829.
13. Legault L-M, Breton-Larrivée M, Langford-Avelar A, Lemieux A, McGraw S. Sex-specific differences in DNA methylation and gene expression in late-gestation mouse placentas. *bioRxiv.* 2023:2023.2009.2023.559106.
14. Coan PM, Burton GJ, Ferguson-Smith AC. Imprinted genes in the placenta--a review. *Placenta.* 2005;26 Suppl A:S10-20.
15. Proudhon C, Bourc'his D. Identification and resolution of artifacts in the interpretation of imprinted gene expression. *Briefings in functional genomics.* 2010;9(5-6):374-384.
16. Wang X, Soloway PD, Clark AG. A survey for novel imprinted genes in the mouse placenta by mRNA-seq. *Genetics.* 2011;189(1):109-122.
17. Lefebvre L. The placental imprintome and imprinted gene function in the trophoblast glycogen cell lineage. *Reproductive biomedicine online.* 2012;25(1):44-57.
18. Golding MC, Magri LS, Zhang L, Lalone SA, Higgins MJ, Mann MR. Depletion of Kcnq1ot1 non-coding RNA does not affect imprinting maintenance in stem cells. *Development (Cambridge, England).* 2011;138(17):3667-3678.
19. Okae H, Hiura H, Nishida Y, et al. Re-investigation and RNA sequencing-based identification of genes with placenta-specific imprinted expression. *Human molecular genetics.* 2012;21(3):548-558.

20. Christians JK, Ahmadzadeh-Seddeighi S, Bilal A, et al. Sex differences in the effects of prematurity and/or low birthweight on neurodevelopmental outcomes: systematic review and meta-analyses. *Biology of sex differences.* 2023;14(1):47.
21. Meakin AS, Cuffe JSM, Darby JRT, Morrison JL, Clifton VL. Let's Talk about Placental Sex, Baby: Understanding Mechanisms That Drive Female- and Male-Specific Fetal Growth and Developmental Outcomes. *International journal of molecular sciences.* 2021;22(12).
22. Bale TL. The placenta and neurodevelopment: sex differences in prenatal vulnerability. *Dialogues in clinical neuroscience.* 2016;18(4):459-464.
23. Martinez-Fierro ML, Garza-Veloz I, Castañeda-Lopez ME, et al. Evaluation of the Effect of the Fibroblast Growth Factor Type 2 (FGF-2) Administration on Placental Gene Expression in a Murine Model of Preeclampsia Induced by L-NAME. *International journal of molecular sciences.* 2022;23(17).
24. Marwa BA, Raguema N, Zitouni H, et al. FGF1 and FGF2 mutations in preeclampsia and related features. *Placenta.* 2016;43:81-85.
25. Bursztyn M, Gross ML, Goltser-Dubner T, et al. Adult hypertension in intrauterine growth-restricted offspring of hyperinsulinemic rats: evidence of subtle renal damage. *Hypertension (Dallas, Tex : 1979).* 2006;48(4):717-723.
26. Plasschaert RN, Bartolomei MS. Genomic imprinting in development, growth, behavior and stem cells. *Development (Cambridge, England).* 2014;141(9):1805-1813.
27. Hemberger M, Cross JC. Genes governing placental development. *Trends in endocrinology and metabolism: TEM.* 2001;12(4):162-168.
28. Apicella C, Ruano CSM, Méhats C, Miralles F, Vaiman D. The Role of Epigenetics in Placental Development and the Etiology of Preeclampsia. *International journal of molecular sciences.* 2019;20(11).
29. Sleutels F, Tjon G, Ludwig T, Barlow DP. Imprinted silencing of Slc22a2 and Slc22a3 does not need transcriptional overlap between Igf2r and Air. *The EMBO journal.* 2003;22(14):3696-3704.
30. Haycock PC, Ramsay M. Exposure of mouse embryos to ethanol during preimplantation development: effect on DNA methylation in the h19 imprinting control region. *Biology of reproduction.* 2009;81(4):618-627.
31. Bourc'his D, Xu GL, Lin CS, Bollman B, Bestor TH. Dnmt3L and the establishment of maternal genomic imprints. *Science (New York, NY).* 2001;294(5551):2536-2539.
32. Logan PC, Mitchell MD, Lobie PE. DNA methyltransferases and TETs in the regulation of differentiation and invasiveness of extra-villous trophoblasts. *Frontiers in genetics.* 2013;4:265.
33. Joh K. Transcription-dependent DNA methylation at the imprinted Zrsr1-DMR. *bioRxiv.* 2018:249524.
34. Arima T, Hata K, Tanaka S, et al. Loss of the maternal imprint in Dnmt3Lmat-/- mice leads to a differentiation defect in the extraembryonic tissue. *Developmental biology.* 2006;297(2):361-373.
35. Andrews S, Krueger C, Mellado-Lopez M, et al. Mechanisms and function of de novo DNA methylation in placental development reveals an essential role for DNMT3B. *Nature communications.* 2023;14(1):371.
36. Rosenfeld CS. The placenta-brain-axis. *Journal of neuroscience research.* 2021;99(1):271-283.
37. Lim J, Tai HH, Liao WH, et al. ASIC1a is required for neuronal activation via low-intensity ultrasound stimulation in mouse brain. *eLife.* 2021;10.
38. McCormick LE, Gupton SL. Cerebellin-1 leads the way. *PLoS biology.* 2022;20(11):e3001880.

39. Seeburg DP, Sheng M. Activity-induced Polo-like kinase 2 is required for homeostatic plasticity of hippocampal neurons during epileptiform activity. *The Journal of neuroscience : the official journal of the Society for Neuroscience.* 2008;28(26):6583-6591.
40. Rosenfeld CS. Placental serotonin signaling, pregnancy outcomes, and regulation of fetal brain development†. *Biology of reproduction.* 2020;102(3):532-538.
41. Frank JW, Steinhauser CB, Wang X, Burghardt RC, Bazer FW, Johnson GA. Loss of ITGB3 in ovine conceptuses decreases conceptus expression of NOS3 and SPP1: implications for the developing placental vasculature†. *Biology of reproduction.* 2021;104(3):657-668.
42. Whyte A, Jessen T, Varney S, Carneiro AM. Serotonin transporter and integrin beta 3 genes interact to modulate serotonin uptake in mouse brain. *Neurochemistry international.* 2014;73:122-126.
43. Bacq A, Balasse L, Biala G, et al. Organic cation transporter 2 controls brain norepinephrine and serotonin clearance and antidepressant response. *Molecular psychiatry.* 2012;17(9):926-939.
44. Laufer BI, Kapalanga J, Castellani CA, Diehl EJ, Yan L, Singh SM. Associative DNA methylation changes in children with prenatal alcohol exposure. *Epigenomics.* 2015;7(8):1259-1274.
45. Portales-Casamar E, Lussier AA, Jones MJ, et al. DNA methylation signature of human fetal alcohol spectrum disorder. *Epigenetics & chromatin.* 2016;9:25.
46. Lussier AA, Morin AM, MacIsaac JL, et al. DNA methylation as a predictor of fetal alcohol spectrum disorder. *Clinical epigenetics.* 2018;10:5.
47. Laufer BI, Neier K, Valenzuela AE, et al. Placenta and fetal brain share a neurodevelopmental disorder DNA methylation profile in a mouse model of prenatal PCB exposure. *Cell reports.* 2022;38(9):110442.
48. Bourgey M, Dali R, Eveleigh R, et al. GenPipes: an open-source framework for distributed and scalable genomic analyses. *GigaScience.* 2019;8(6).
49. Krueger F, Andrews SR. Bismark: a flexible aligner and methylation caller for Bisulfite-Seq applications. *Bioinformatics (Oxford, England).* 2011;27(11):1571-1572.
50. Akalin A, Kormaksson M, Li S, et al. methylKit: a comprehensive R package for the analysis of genome-wide DNA methylation profiles. *Genome biology.* 2012;13(10):R87.
51. Legault LM, Doiron K, Lemieux A, et al. Developmental genome-wide DNA methylation asymmetry between mouse placenta and embryo. *Epigenetics.* 2020;15(8):800-815.
52. Heinz S, Benner C, Spann N, et al. Simple combinations of lineage-determining transcription factors prime cis-regulatory elements required for macrophage and B cell identities. *Molecular cell.* 2010;38(4):576-589.
53. Zhou Y, Zhou B, Pache L, et al. Metascape provides a biologist-oriented resource for the analysis of systems-level datasets. *Nature communications.* 2019;10(1):1523.
54. Karolchik D, Hinrichs AS, Furey TS, et al. The UCSC Table Browser data retrieval tool. *Nucleic acids research.* 2004;32(Database issue):D493-496.
55. Bolger AM, Lohse M, Usadel B. Trimmomatic: a flexible trimmer for Illumina sequence data. *Bioinformatics (Oxford, England).* 2014;30(15):2114-2120.
56. Dobin A, Davis CA, Schlesinger F, et al. STAR: ultrafast universal RNA-seq aligner. *Bioinformatics (Oxford, England).* 2013;29(1):15-21.
57. Li H, Durbin R. Fast and accurate short read alignment with Burrows-Wheeler transform. *Bioinformatics (Oxford, England).* 2009;25(14):1754-1760.
58. Love MI, Huber W, Anders S. Moderated estimation of fold change and dispersion for RNA-seq data with DESeq2. *Genome biology.* 2014;15(12):550.

59. Xu Y, Wang X, Huang Y, Ye D, Chi P. A LASSO-based survival prediction model for patients with synchronous colorectal carcinomas based on SEER. *Translational cancer research.* 2022;11(8):2795-2809.
60. Sohn I, Kim J, Jung SH, Park C. Gradient lasso for Cox proportional hazards model. *Bioinformatics (Oxford, England).* 2009;25(14):1775-1781.
61. Taft LM, Evans RS, Shyu CR, et al. Countering imbalanced datasets to improve adverse drug event predictive models in labor and delivery. *Journal of biomedical informatics.* 2009;42(2):356-364.

**TABLES**

**Table 1: Top 10 sex-specific DMRs**

| Male-specific DMRs | | | |
|---|---|---|---|
| **Effect of EtOH exposure** | **Gene symbol** | **Methylation change (%)** | **Annotation** |
| Decreased | *(Hmox2)* | -33.13 | Intergenic |
| Decreased | *Trappc9* | -31.79 | Intron |
| Decreased | *Arsg* | -28.90 | Intron |
| Decreased | *Mir148b* | -28.61 | Intron |
| Decreased | *(Cplx2)* | -28.02 | Intergenic |
| Decreased | *Mrpl45* | -27.29 | 3′ UTR |
| Decreased | *(Slc1a5)* | -26.62 | Intergenic |
| Decreased | *(Cdh15)* | -26.58 | Intergenic |
| Decreased | *a (agouti)* | -26.54 | Intron |
| Decreased | *Cacna2d3* | -25.99 | Intron |
| Increased | *Snai2* | 36.27 | Intron |
| Increased | *Egln3* | 29.58 | Intron |
| Increased | *(Ctrc)* | 28.57 | Intergenic |
| Increased | *(Snai1)* | 28.13 | Intergenic |
| Increased | *Pik3r4* | 27.20 | Exon |
| Increased | *Me1* | 27.06 | Intron |
| Increased | *Rubcnl* | 26.94 | Intron |
| Increased | *(Chrna5)* | 26.47 | Intergenic |

| | | | |
|---|---|---|---|
| Increased | *Ilf3* | 25.76 | 3′ UTR |
| Increased | *(Tmem150cos)* | 25.49 | Intergenic |
| **Female-specific DMRs** | | | |
| **Effect of EtOH exposure** | **Gene symbol** | **Methylation change (%)** | **Annotation** |
| Decreased | *(Pla2g4d)* | -39.54 | Intergenic |
| Decreased | *Mfsd2a* | -37.35 | Intron |
| Decreased | *Pygo1* | -31.79 | Intron |
| Decreased | *(Plau)* | -29.63 | Intergenic |
| Decreased | *(Jun)* | -29.28 | Intergenic |
| Decreased | *Msx1os* | -28.73 | Non-coding |
| Decreased | *(Zfp57)* | -28.31 | Intergenic |
| Decreased | *Capza2* | -26.06 | Intron |
| Decreased | *(Hpf1)* | -25.90 | Intergenic |
| Decreased | *Traf6* | -25.16 | Intron |
| Increased | *(Ssbp3)* | 37.50 | Intergenic |
| Increased | *Jdp2* | 34.63 | TTS |
| Increased | *(Sox5os3)* | 33.91 | Intergenic |
| Increased | *(Fam98b)* | 32.86 | Intergenic |
| Increased | *(Usp7)* | 32.66 | Intergenic |
| Increased | *Fgf12* | 32.61 | Intron |
| Increased | *(Kpna1)* | 32.06 | Intergenic |
| Increased | *Fam105a* | 31.71 | Intron |

| | | | |
|---|---|---|---|
| Increased | *(Ppif)* | 30.73 | Intergenic |
| Increased | *(Pax9)* | 30.45 | Intergenic |

**Table 2: Top 10 shared DMRs between male and female placentas**

| Shared top DMRs | | | | | |
|---|---|---|---|---|---|
| **Effect of EtOH (males)** | **Gene symbol** | **Methylation change (%) (males)** | **Effect of EtOH (females)** | **Methylation change (%) (females)** | **Annotation** |
| *Cdk8* | Decreased | -23.33 | Decreased | -12.21 | Intron |
| (*Mirt1*) | Decreased | -13.04 | Decreased | -12.24 | Intergenic |
| *Hs3st2* | Decreased | -12.54 | Decreased | -10.83 | Exon |
| *Tmem267* | Decreased | -12.51 | Decreased | -10.67 | Promoter-TSS |
| *Rbm3os* | Decreased | -10.07 | Increased | 15.50 | Promoter-TSS |
| (*Ifngas1*) | Increased | 15.22 | Decreased | -20.68 | Intergenic |
| (*Slc22a19*) | Increased | 10.02 | Decreased | -10.61 | Intergenic |
| *Tro* | Increased | 10.12 | Increased | 13.77 | Promoter-TSS |
| *Galp* | Increased | 15.12 | Increased | 10.21 | Exon |
| (*Spry1*) | Increased | 15.01 | Increased | 15.70 | Intergenic |
| *Clstn3* | Increased | 13.36 | Increased | 15.06 | Exon |
| (*Spry1*) | Increased | 13.08 | Increased | 12.83 | Intergenic |

| | | | | | |
|---|---|---|---|---|---|
| *Spry1* | Increased | 13.00 | Increased | 16.15 | Intergenic |
| (*Spry1*) | Increased | 12.05 | Increased | 11.63 | Intergenic |
| *Socs5* | Increased | 11.55 | Increased | 13.67 | Intron |
| *Psd3* | Increased | 11.40 | Increased | 10.02 | Intron |
| *Socs5* | Increased | 11.02 | Increased | 11.20 | Exon |
| *Wwox* | Increased | 10.80 | Increased | 10.94 | Intron |
| *Trh* | Increased | 10.18 | Increased | 11.33 | Intergenic |

**Table 3: Top 10 decreased and increased sex-specific DEGs**

| **Male-specific DEGs** | | | |
|---|---|---|---|
| **Condition** | **Gene symbol** | **Log2 fold change** | ***p*-value** |
| Decreased | *Ear1* | -5.66 | 0.04 |
| Decreased | *Klk15* | -4.67 | 0.001 |
| Decreased | *Kap* | -4.31 | 0.01 |
| Decreased | *Ang2* | -4.03 | 0.05 |
| Decreased | *Pcdhb8* | -3.93 | 0.04 |
| Decreased | *Jsrp1* | -3.74 | 0.01 |
| Decreased | *Cdc20b* | -3.64 | 0.04 |
| Decreased | *Aadacl3* | -3.53 | 0.04 |
| Decreased | *Shisa3* | -3.11 | 0.01 |
| Decreased | *Crabp1* | -3.05 | 0.001 |
| Increased | *Lrrc4b* | 4.38 | 0.01 |
| Increased | *C8a* | 3.51 | 0.01 |

| | | | |
|---|---|---|---|
| Increased | *Alb* | 3.43 | 0.02 |
| Increased | *Krt77* | 3.34 | 0.04 |
| Increased | *Gria1* | 3.24 | 0.03 |
| Increased | *Stmn3* | 3.08 | 0.03 |
| Increased | *Fgg* | 3.03 | 0.02 |
| Increased | *Trpm2* | 2.95 | 0.02 |
| Increased | *Spink3* | 2.94 | 0.03 |
| Increased | *Krt6b* | 2.93 | 0.01 |
| **Female-specific DEGs** | | | |
| **Condition** | **Gene symbol** | **Log2 fold change** | ***p*-value** |
| Decreased | *Ddn* | -3.88 | 0.04 |
| Decreased | *Caly* | -3.86 | 0.04 |
| Decreased | *Serpinb2* | -2.89 | 0.01 |
| Decreased | *Dsc1* | -2.81 | 0.01 |
| Decreased | *Cyp2b19* | -2.63 | 0.003 |
| Decreased | *Cyp2ab1* | -2.46 | 0.02 |
| Decreased | *Dsg3* | -1.96 | 0.002 |
| Decreased | *Serpina3c* | -1.96 | 0.04 |
| Decreased | *Nol4* | -1.86 | 0.05 |
| Decreased | *Marco* | -1.74 | 0.03 |
| Increased | *Serpina1c* | 4.96 | 0.003 |
| Increased | *Mir296* | 4.73 | 0.001 |
| Increased | *Oprm1* | 4.06 | 0.03 |

| | | | |
|---|---|---|---|
| Increased | *Klk1b8* | 4.06 | 0.02 |
| Increased | *Fgf23* | 4.04 | 0.04 |
| Increased | *Dmrt3* | 3.86 | 0.03 |
| Increased | *St6galnac1* | 3.67 | 0.05 |
| Increased | *Myot* | 3.24 | 0.05 |
| Increased | *C6* | 3.10 | 0.03 |
| Increased | *Pigr* | 3.08 | 0.02 |

**Table 4: Top 10 shared DEGs**

| **Shared top DEGs** | | | | | | |
|---|---|---|---|---|---|---|
| **Effect of EtOH (males)** | **Gene symbol** | **Log2 fold change (males)** | ***p*-value (males)** | **Effect of EtOH (females)** | **Log2 fold change (females)** | ***p*-value (females)** |
| Decreased | *Dok7* | -0.92 | 0.00 | Decreased | -0.60 | 0.03 |
| Decreased | *Spata2l* | -0.36 | 0.04 | Decreased | -0.39 | 0.04 |
| Decreased | *Foxf2* | -0.55 | 0.03 | Decreased | -0.38 | 0.02 |
| Decreased | *Chchd10* | -0.41 | 0.01 | Decreased | -0.33 | 0.01 |
| Decreased | *Timp2* | -0.44 | 0.04 | Decreased | -0.33 | 0.01 |
| Decreased | *Gpr156* | -0.52 | 0.01 | Decreased | -0.33 | 0.01 |
| Decreased | *Map2k6* | -0.37 | 0.02 | Decreased | -0.31 | 0.05 |
| Decreased | *St8sia5* | -0.61 | 0.00 | Decreased | -0.29 | 0.04 |
| Decreased | *Ypel3* | -0.32 | 0.00 | Decreased | -0.23 | 0.03 |
| Decreased | *Ifit2* | -0.43 | 0.02 | Increased | 0.33 | 0.04 |

| | | | | | | |
|---|---|---|---|---|---|---|
| Increased | *Dsc3* | 1.74 | 0.05 | Decreased | -2.10 | 0.03 |
| Increased | *Dnajc6* | 1.22 | 0.03 | Increased | 0.87 | 0.04 |
| Increased | *Syt14* | 0.60 | 0.00 | Increased | 0.60 | 0.01 |
| Increased | *Pm20d1* | 0.51 | 0.01 | Increased | 0.55 | 0.004 |
| Increased | *Tceal7* | 0.50 | 0.02 | Increased | 0.51 | 0.01 |
| Increased | *Pdzk1ip1* | 0.69 | 0.00 | Increased | 0.47 | 0.04 |
| Increased | *Serpinb1a* | 0.59 | 0.03 | Increased | 0.46 | 0.02 |
| Increased | *Musk* | 0.54 | 0.00 | Increased | 0.40 | 0.04 |
| Increased | *Gsta3* | 0.64 | 0.01 | Increased | 0.40 | 0.04 |
| Increased | *Scel* | 0.53 | 0.00 | Increased | 0.28 | 0.04 |

## FIGURES and LEGENDS

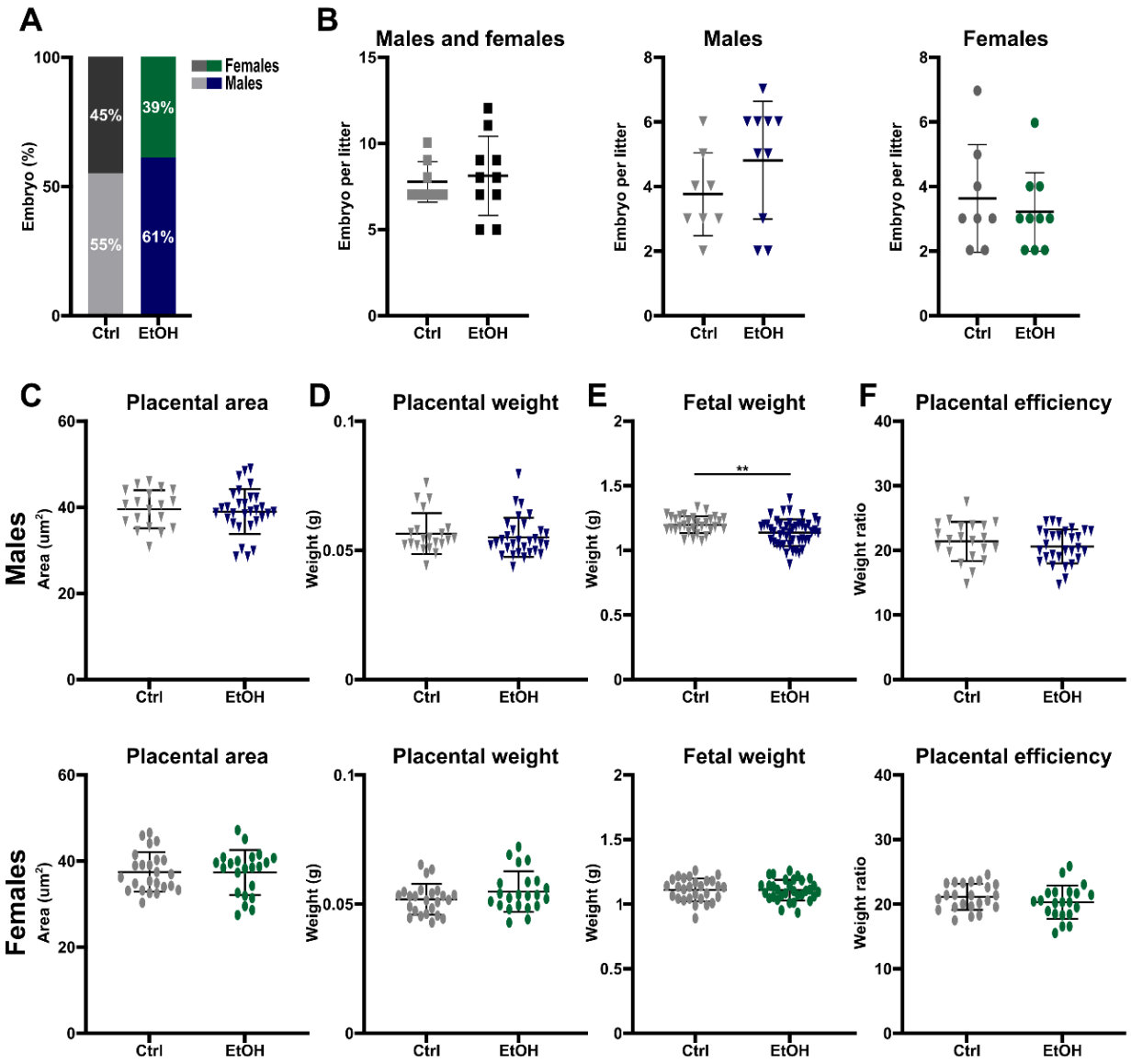


**Figure 1: Absence of morphometric alterations in E18.5 placentas following preimplantation alcohol exposure**

**A)** Sex ratios of litters (control: males *n*=47, females *n*=39; ethanol-exposed: males *n*=62, females *n*=39) shown as percentages. **B)** E18.5 embryos per litter in the control (*n*=8 litters; average 7.75 embryos/litter) and ethanol-exposed (*n*=10 litters; average 8.10 embryos/litter) groups. Number of male embryos per litter in the control (*n*=8 litters; average 3.75 embryos/litter) and ethanol-exposed (*n*=10 litters; average

4.80 embryos/litter) groups. Number of female embryos per litter in the control (*n*=8 litters; average 3.63 embryos/litter) and ethanol-exposed (*n*=10 litters; average 3.20 embryos/litter) groups. **C)** Placental surface area measurements in males and females at E18.5 (control embryos: males, *n*=19, 6 litters; females, *n*=24, 6 litters; ethanol-exposed embryos: males *n*=30, 6 litters; females, *n*=22, 6 litters). **D)** Placental weight in males and females at E18.5 (control embryos: males, *n*=19, 6 litters; females, *n*=24, 6 litters; ethanol-exposed embryos: males, *n*=30, 6 litters; females, *n*=22, 6 litters). **E)** Fetal weight in males and females at E18.5 (control embryos: males, *n*=31, 8 litters; females, *n*=28, 8 litters; ethanol-exposed embryos: males, n=46, 10 litters; females, *n*=32, 8 litters). **F)** Placental efficiency (fetal-to-placental weight ratio) in males and females) at E18.5 (control embryos: males, *n*=19, 6 litters; females, *n*=24, 6 litters; ethanol-exposed embryos: males, *n*=30, 6 litters; females, *n*=22, 6 litters). All data represent the mean ± standard deviation (SD). Significant differences were assessed by *t*-test with Welch's correction. **: $p<0.01$.

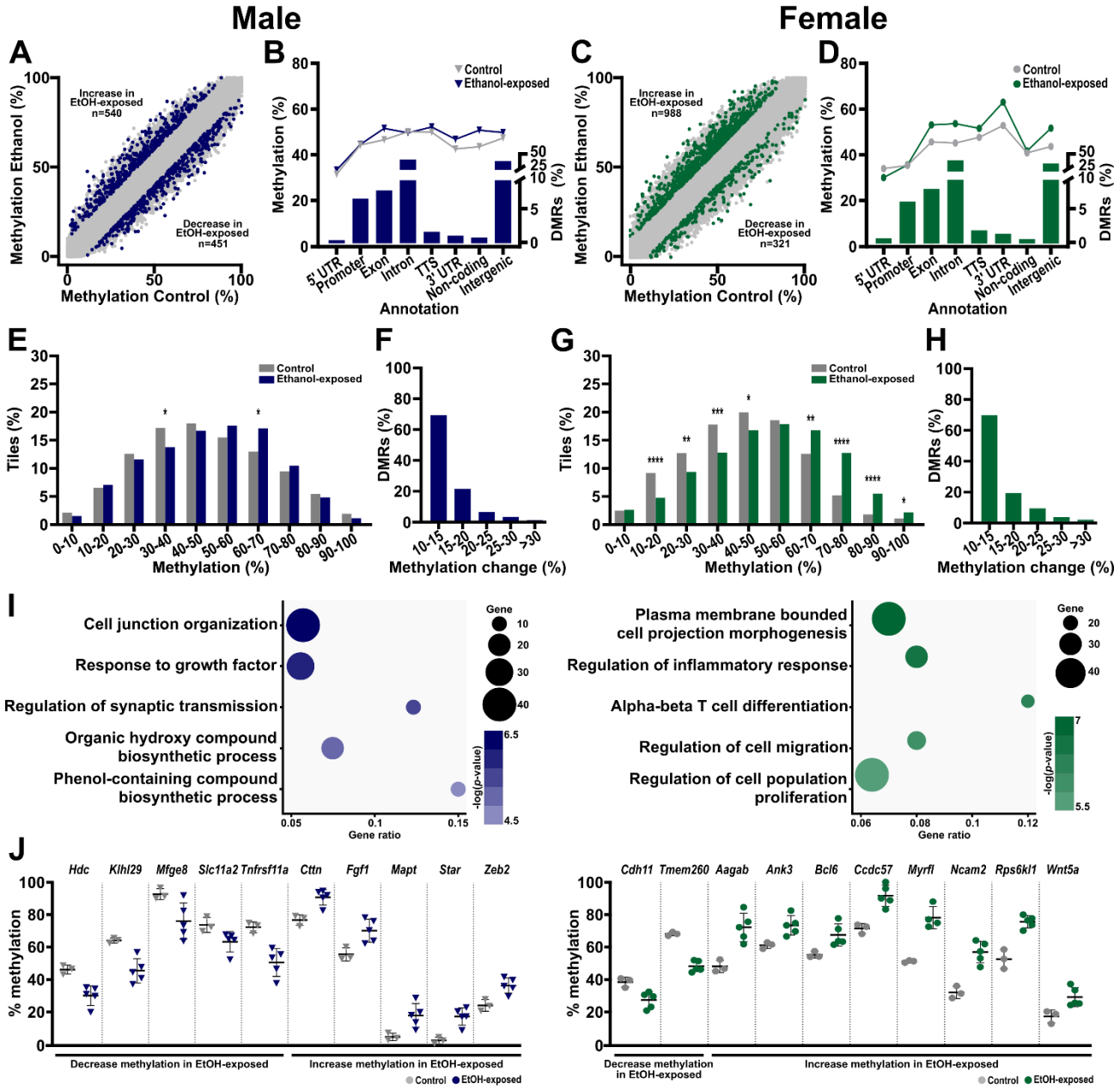


**Figure 2: Sex-specific DNA methylation dysregulation in the placenta following early preimplantation alcohol exposure**

**A)** Scatterplot of differentially methylated regions (DMRs) between control and ethanol-exposed male placentas. Blue dots represent tiles with ≥ 10% methylation changes in ethanol-exposed placentas compared to controls (*n*=991). **B)** CpG methylation levels in control and ethanol-exposed male placentas based on DMR annotations (left Y-axis) and DMR distributions across genomic annotations (right Y-

axis). **C)** Scatterplot of DMRs between control and ethanol-exposed female placentas. Green dots represent tiles with ≥ 10% methylation changes in ethanol-exposed placentas compared to controls (*n*=1309). **D)** CpG methylation levels in control and ethanol-exposed female placentas based on DMR annotations (left Y-axis) and DMR distributions across genomic annotations (right Y-axis). **E)** Tile distributions across DNA methylation levels in male-specific control and ethanol-exposed DMRs (*n*=991). **F)** Proportion of male DMRs (*n*=991) associated with changes in CpG methylation levels between control and ethanol-exposed placentas. **G)** Tile distributions across DNA methylation levels in female-specific control and ethanol-exposed DMRs (*n*=1309). **H)** Proportion of female DMRs (*n*=1309) associated with changes in CpG methylation levels between control and ethanol-exposed placentas. **I)** Top enriched pathways in male (*n*=542 unique gene DMRs; left, blue) and female (*n*=749 unique gene DMRs; right, green) DMRs based on Metascape analysis. **J)** CpG methylation levels of top changed DMRs or DMRs associated with the top enriched pathways shown in **I** in control and ethanol-exposed male (left; grey/blue) and female (right; grey/green) placentas. Data represent the mean ± SD.

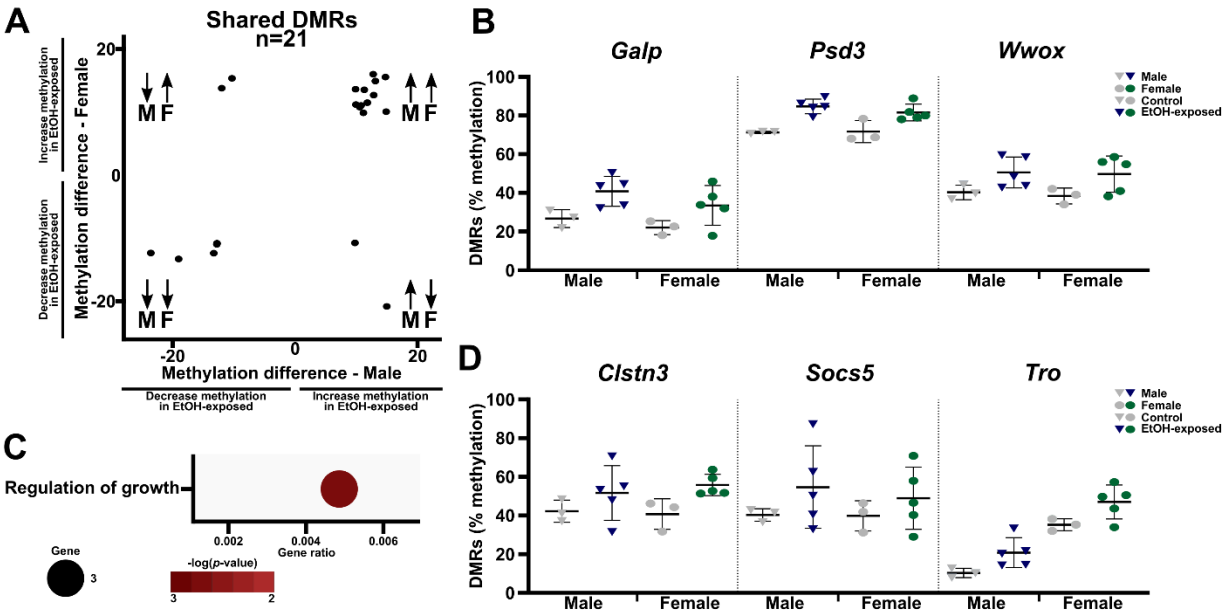


**Figure 3: Regions presenting shared differential DNA methylation patterns in ethanol-exposed male and female placentas are enriched in genes related to growth**

**A)** Percentage of change in in the 21 shared DMRs in males and females. **B)** CpG methylation levels of shared DMRs in control and ethanol-exposed male (left; grey/blue) and female (right; grey/green) placentas. **C)** Top pathways enriched for shared DMRs (*n*=11 unique gene DMRs) based on Metascape analysis. **D)** CpG methylation levels for DMRs located in enriched growth-regulating genes (from **C**) in control and ethanol-exposed male (left dots; grey/blue) and female (right dots; grey/green) placentas. Data represent the mean ± SD.

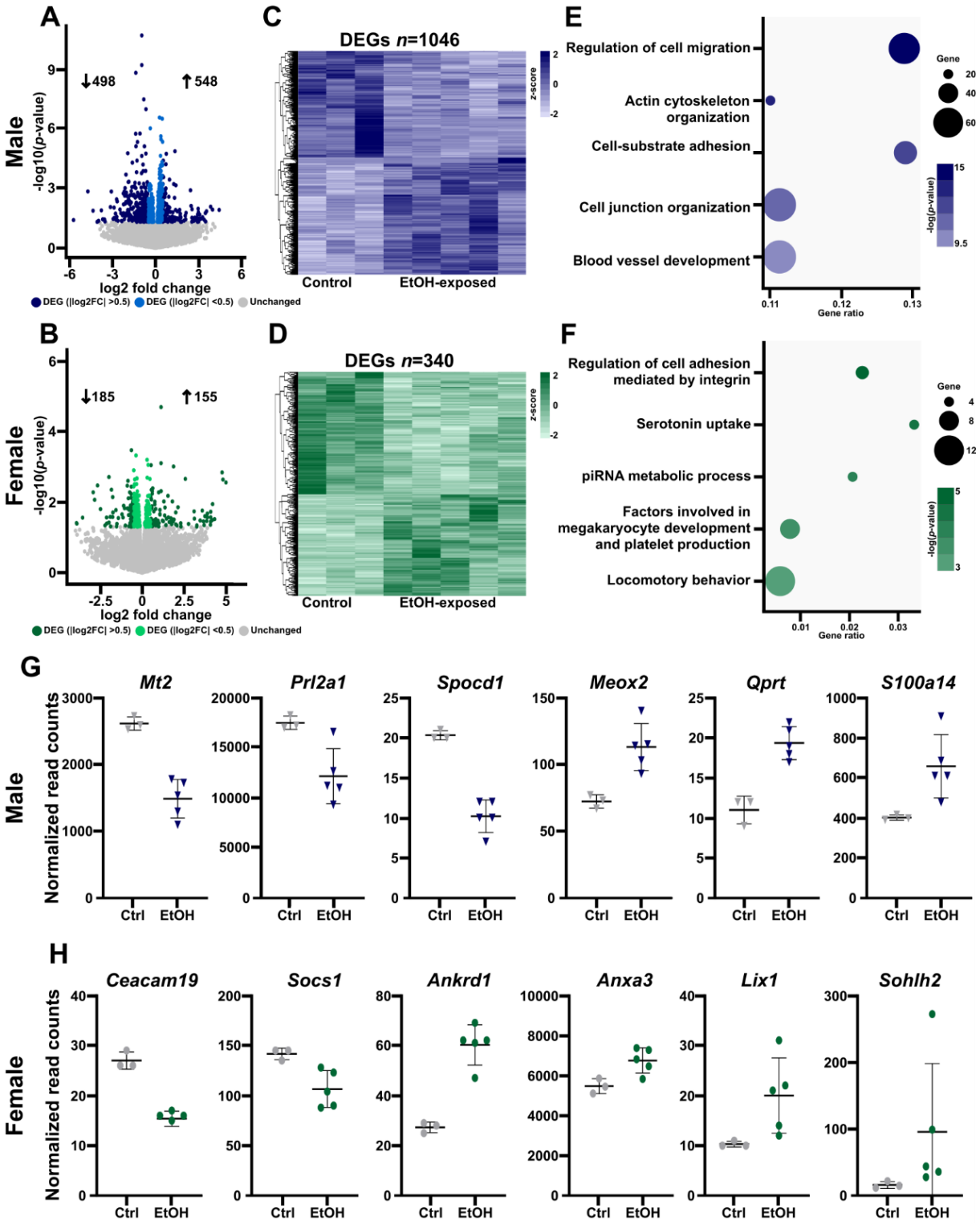


**Figure 4: Gene expression profiles are especially affected in the male placenta following preimplantation alcohol exposure**

**A-B)** Differential expression analyses between control and ethanol-exposed placenta in **A)** and **B)** females. Colored dots represent statistically significant DEGs ($p<0.05$; males, $n=1046$; females, $n=340$). Darker dots represent DEGs with log2 fold change values > 0.5 (males, $n=359$; females, $n=157$). **C-D)** Heatmaps of DEG expression levels (*z*-scores) in control and ethanol-exposed **C)** male and **D)** female placentas. **E-F)** Top pathways for **E)** male ($n=1046$) and **F)** female ($n=340$) DEGs based on Metascape analysis. **G-H)** Normalized read counts of selected DEGs in **G)** male and **H)** female ethanol-exposed placentas. Data represent the mean ± SD.

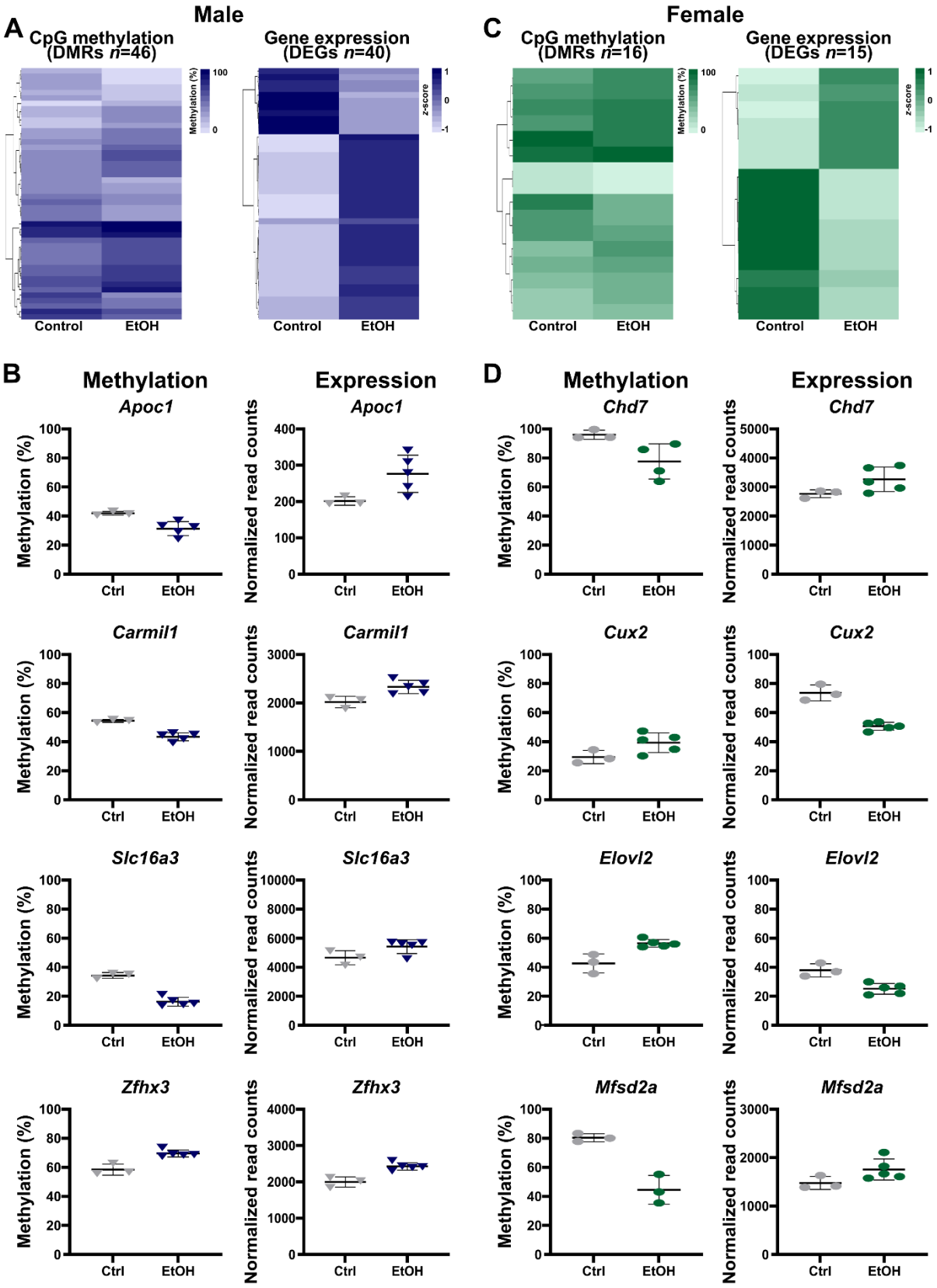
A
Male
CpG methylation (DMRs n=46)
Gene expression (DEGs n=40)
Methylation (%)
z-score
Control
EtOH
C
Female
CpG methylation (DMRs n=16)
Gene expression (DEGs n=15)
B
Methylation
Expression
Apoc1
Carmil1
Slc16a3
Zfhx3
D
Chd7
Cux2
Elovl2
Mfsd2a
Methylation (%)
Normalized read counts
Ctrl
EtOH

**Figure 5: Sex-specific regions show both DNA methylation and gene expression alterations in the placenta at late gestation in response to early preimplantation alcohol exposure**

**A)** Heatmaps of CpG methylation (left) and gene expression (*z*-score; right) levels of DEGs containing intragenic DMRs between control and ethanol-exposed male (*n*= 46 DMRs, *n*=42 DEGs) **B)** Normalized read counts of DEGs and DMRs in male placentas. **C**) Heatmaps of CpG methylation (left) and gene expression (*z*-score; right) levels of DEGs containing intragenic DMRs between control and ethanol-exposed female (*n*=16 DMRs, *n*=15 DEGs) placentas. **D**) Normalized read counts of DEGs and DMRs in female placentas. Data represent the mean ± SD.

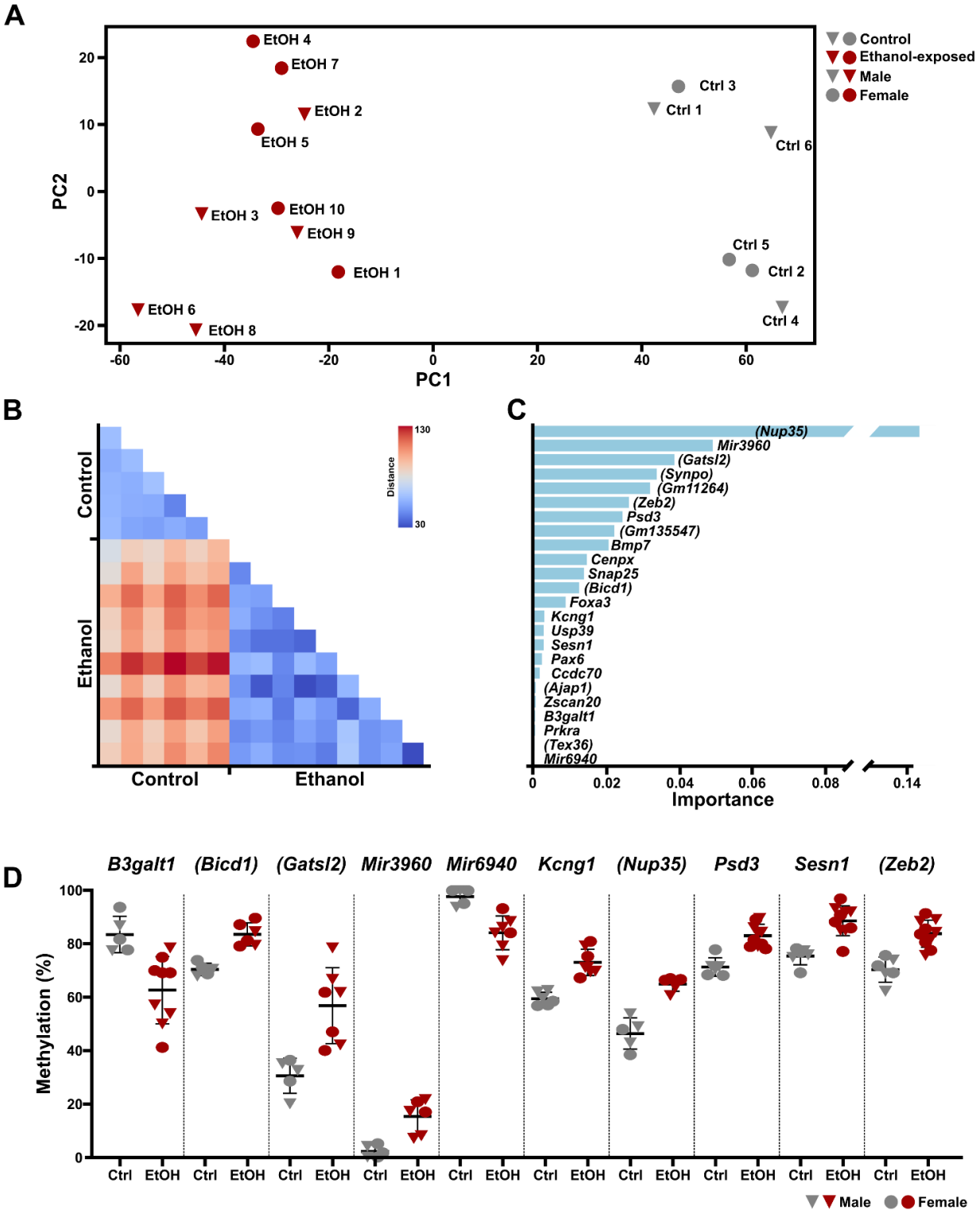


**Figure 6: A signature of dysregulated DNA methylation in the late-gestation placenta as a biomarker of PAE**

**A)** Principal component analysis showing the clustering of control and ethanol-exposed samples based on their CpG methylation levels in the 24 DMRs identified as possible biomarkers. **B)** Heatmap of the Euclidean distances of each control and ethanol-exposed sample based on their CpG methylation levels in the 24 DMRs. **C)** Feature importance plot of the biomarker DMRs based on LASSO analysis. **D)** CpG methylation levels in control and ethanol-exposed male and female placental biomarker DMRs. Genes in brackets are the closest gene to the intergenic DMR.

## SUPPLEMENTAL FIGURES and LEGENDS

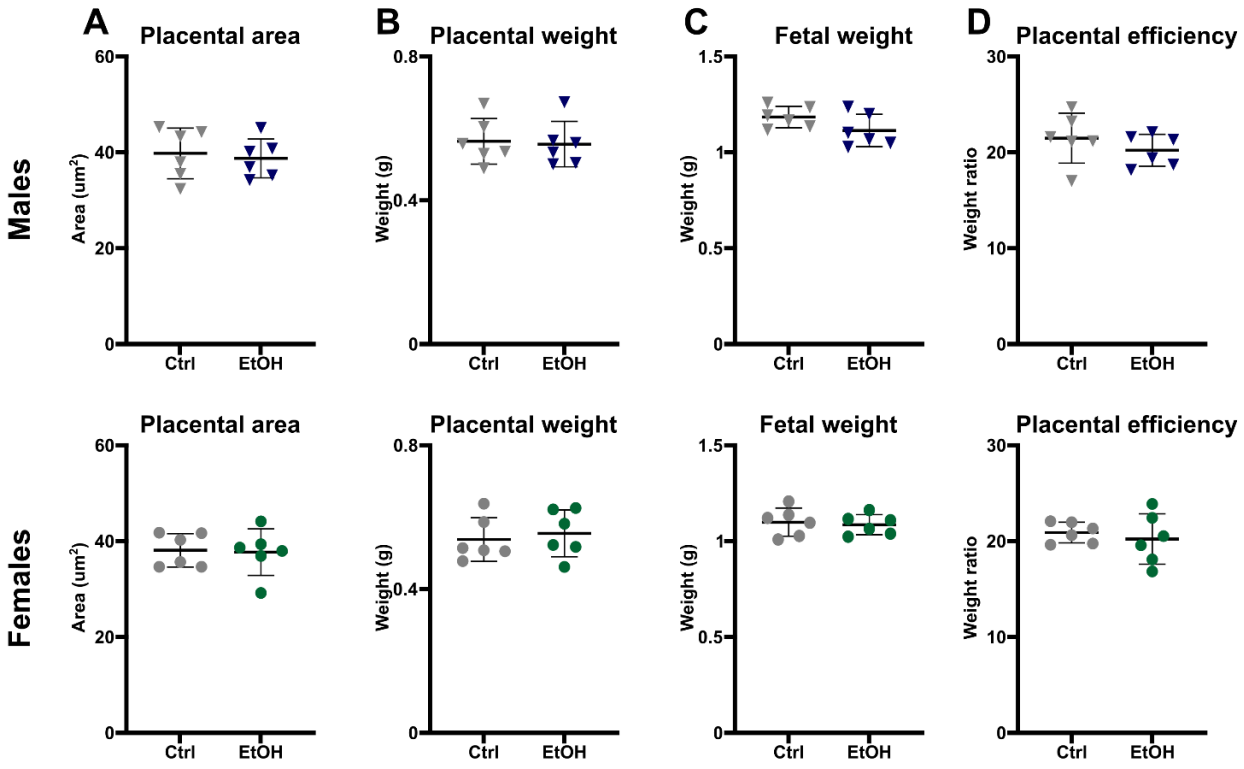


**Supplemental Figure 1: Morphometric measurements of placentas and embryos**

**A)** Average placental surface area measurements per litter in males (top) and females (bottom) at E18.5. (control embryos: males, *n*=2–6 embryos per litter, 6 litters; females, *n*=2–7 embryos per litter, 6 litters; ethanol-exposed embryos: males, *n*=2–7 embryos per litter, 6 litters; females, *n*=2–6 embryos per litter, 6 litters). **B)** Average placental weight per litter in males (top) and females (bottom) at E18.5 (control embryos: males, *n*=2–6 embryos per litter, 6 litters; females, *n*=2–7 embryos per litter, 6 litters; ethanol-exposed embryos: males, *n*=2–7 embryos per litter, 6 litters; females, *n*=2–6 embryos per litter, 6 litters). **C)** Average fetal weight per litter in males (top) and females (bottom) at E18.5 (control embryos: males, *n*=2–6 embryos per litter, 8 litters; females, *n*=2–7 embryos per litter, 8 litters; ethanol-exposed embryos: males, *n*=2–7 embryos per litter, 10 litters; females, *n*=2–6 embryos per litter, 10 litters). **D)** Average placental efficiency per litter (fetal-to-placental weight ratio) in males (top) and females (bottom) at E18.5 (control embryos: males, *n*=2–6 embryos per litter, 6 litters; females, *n*=2–7 embryos per litter, 6

litters; ethanol-exposed embryos: males, *n*=2–7 embryos per litter, 6 litters; females, *n*=2–6 embryos per litter, 6 litters). All data represent the mean ± SD. Significant differences were assessed by *t*-test with Welch's correction.

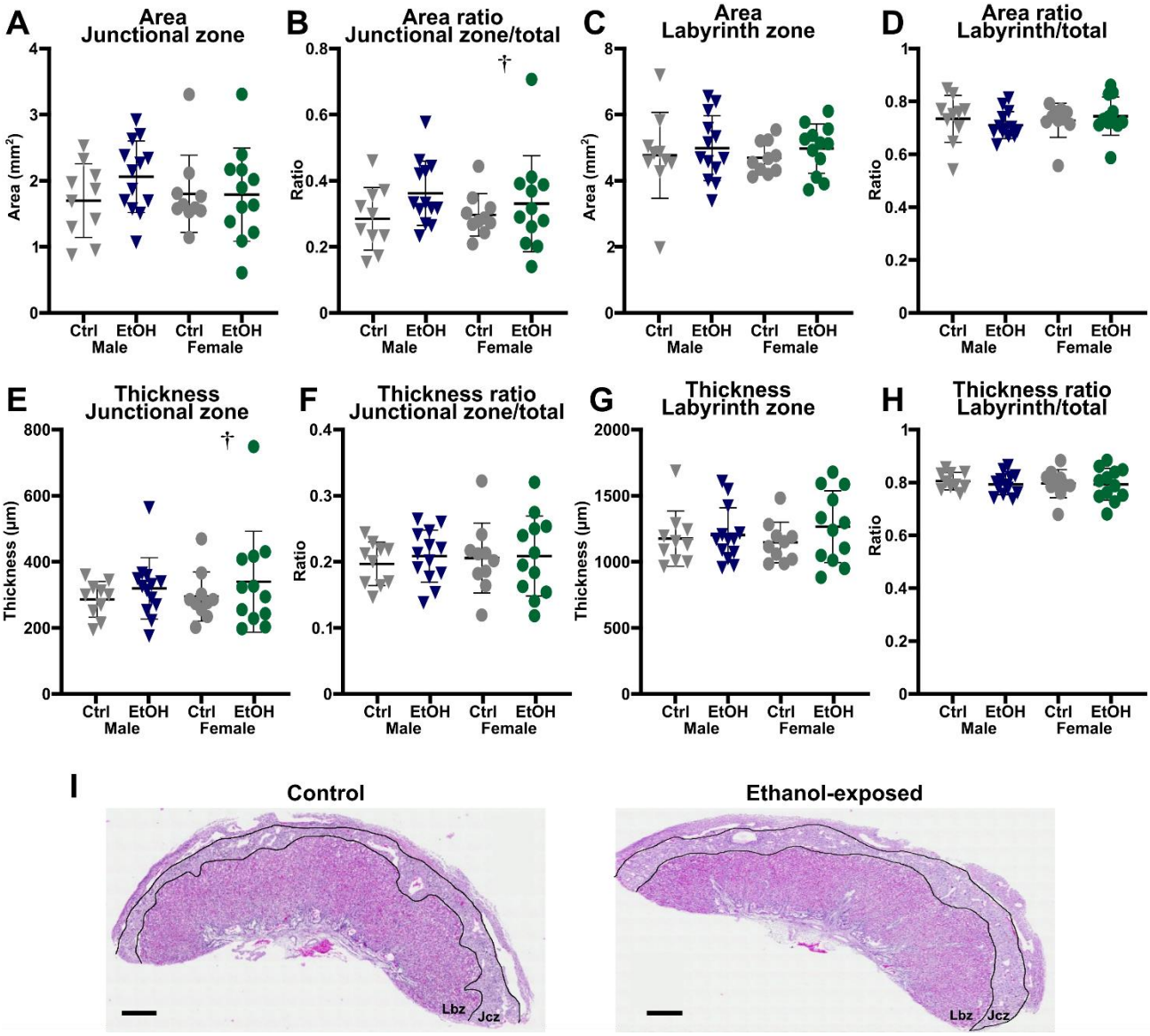


**Supplemental Figure 2: Increased variability in female ethanol-exposed placenta morphometric measurements**

Histological morphometric measurements of E18.5 placentas based on placental cross-sections. **A)** Junctional zone (Jcz) area. **B)** Ratio of the Jcz area to the total placental area. **C)** Labyrinth zone (Lbz) area. **D)** Ratio of the Lbz area to the total placental area. **E)** Thickness of the Jcz. **F)** Ratio of Jcz thickness to the total placental thickness. **G)** Thickness of the Lbz. **H)** Ratio of the Lbz thickness to the total placental thickness. All data represent the mean ± SD. Significant differences were assessed by *t*-test with Welch's correction and *F* tests for the variance analysis. **I)** Representative images of hematoxylin

and eosin-stained control and ethanol-exposed samples. The Jcz and Lbz are delimited by black lines. † Higher variance in ethanol-exposed placentas; *F*-test, $p<0.05$.

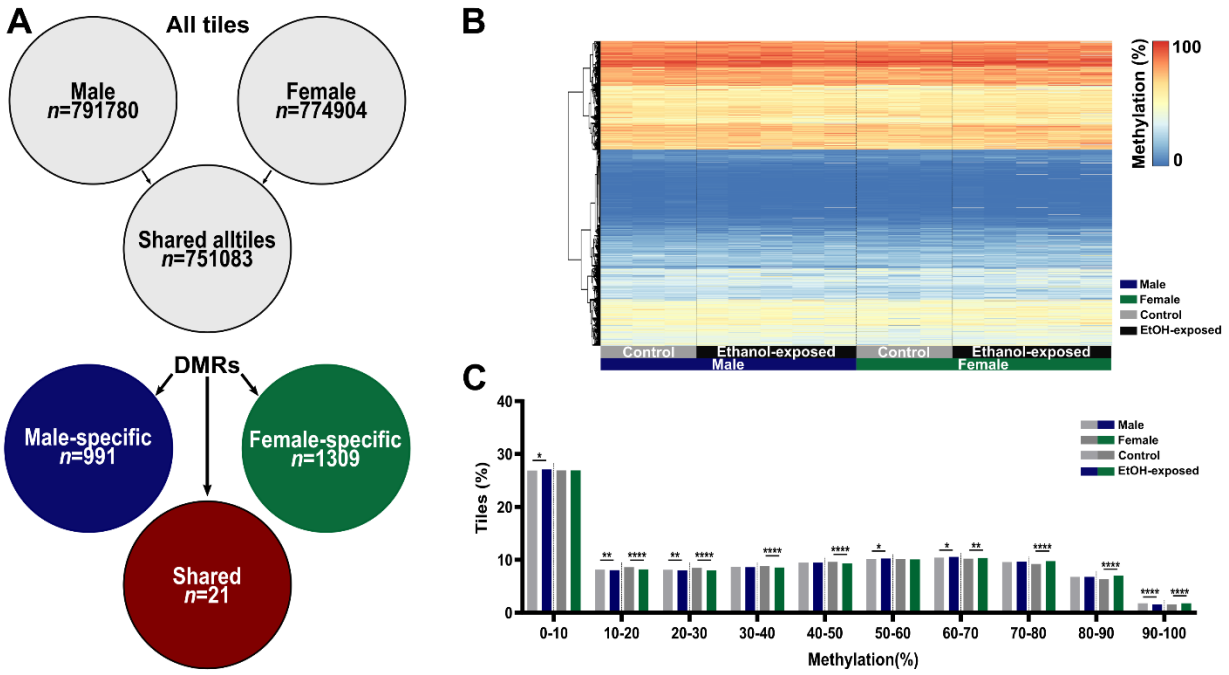


**Supplemental Figure 3: Establishing DNA methylation profiles in alcohol-exposed late-gestation placentas (E18.5)**

**A)** Schematic of the sex-related genome-wide CpG methylation analysis in male (Ctrl, *n*=3; EtOH, *n*=5) and female (Ctrl, *n*=3; EtOH, *n*=5) placentas at E18.5 to identify all tiles associated with either males *n*= 791,780), females (*n*=774,904), or both sexes (*n*=751 083), as well as male-specific (*n*=991), female-specific (*n*=1309), and common (*n*=21) DMRs). **B)** Heatmap of DNA methylation levels in a random subset of tiles (~1% of the 751,083 total tiles; 100 bases, > 10× coverage) from individual male and female control and EtOH-exposed placentas. No clustering has been applied. **C)** Tile distributions across DNA methylation levels in male and female control and ethanol-exposed placentas (shared tiles; *n*=751,083). ****: $p<0.0001$, **: $p<0.01$, *: $p<0.05$ by two-proportions *z*-test test.

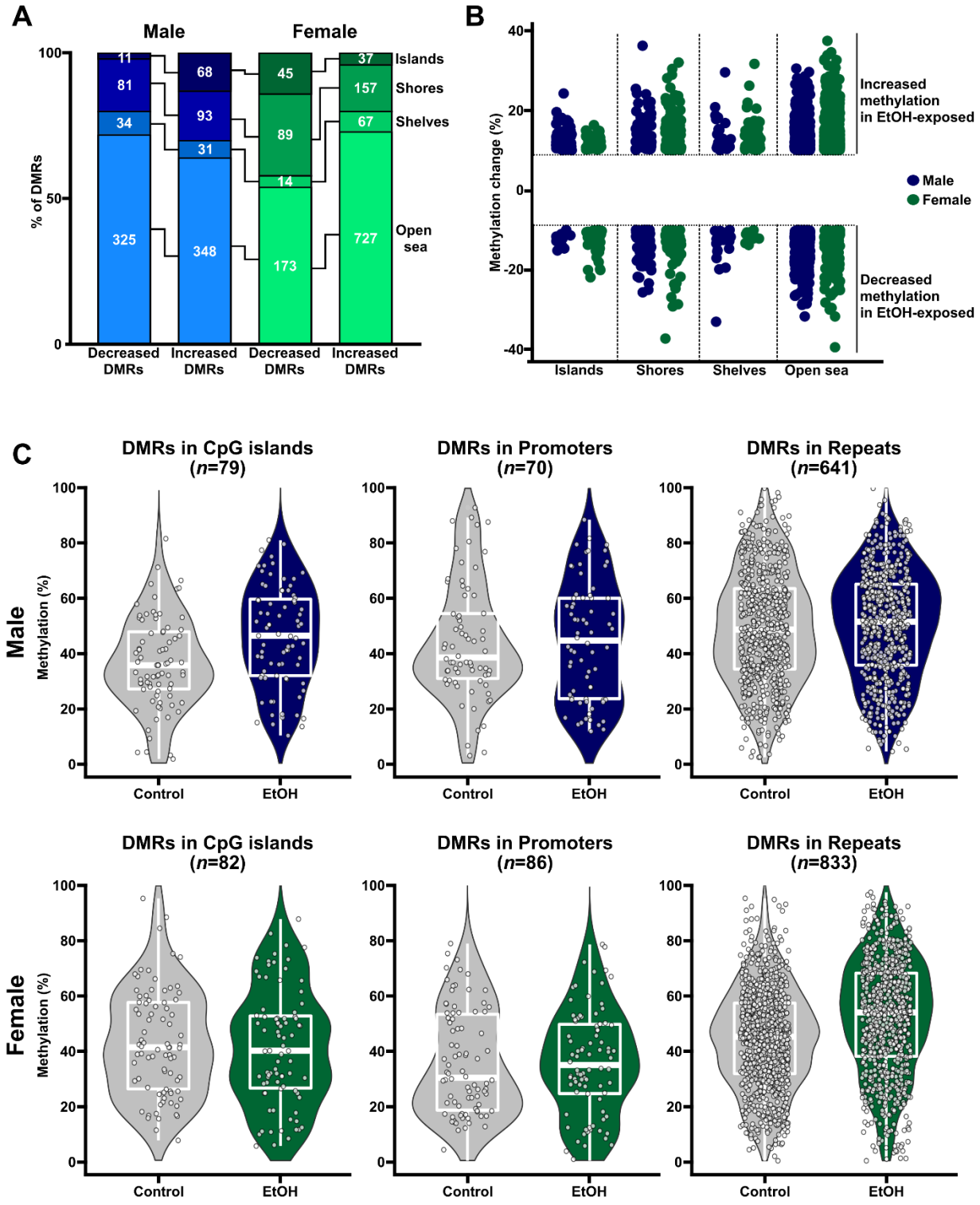


**Supplemental Figure 4: Female ethanol-exposed placentas tend to lose methylation in CpG rich regions**

**A)** Distribution of DMRs between control and ethanol-exposed male (blue) and female (green) placentas based on their proximity to CpG-rich regions (CpG islands (CGIs). Regions are defined as shores (≤ 2 kb from CGIs), shelves (2–4 kb from CGIs), and open sea (≥ 4 kb from CGIs). **B)** Methylation differences in male- (blue) and female- (green) specific DMRs based on their proximities to CGIs. **C)** DNA methylation distributions in different CpG density contexts in males (blue; top) and females (green; bottom).

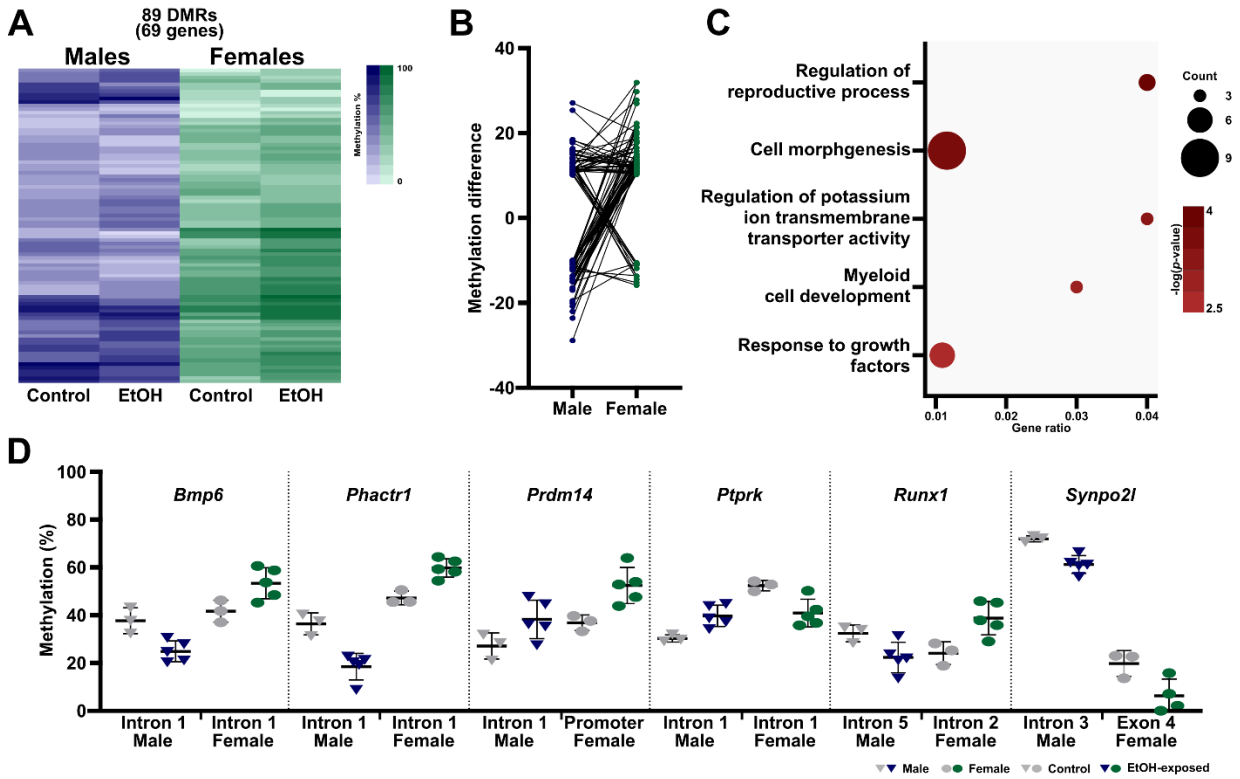


**Supplemental Figure 5: Sex-specific changes in different regions of the same genes in ethanol-exposed placentas**

**A)** Heatmaps of the CpG methylation levels of DMRs within the same genes in male (blue) and female (green) placentas. **B)** Methylation differences between males and females. Connected dots represent DMRs in a shared gene. **C)** Top pathways enriched for shared genes with male and female intragenic DMRs (*n*=69 unique genes) based on Metascape analysis. **D)** CpG methylation levels of DMRs located in genes related to top enriched pathways in control and ethanol-exposed male (left dots; grey/blue) and female (right dots; grey/green) placentas. Data represent the mean ± SD.

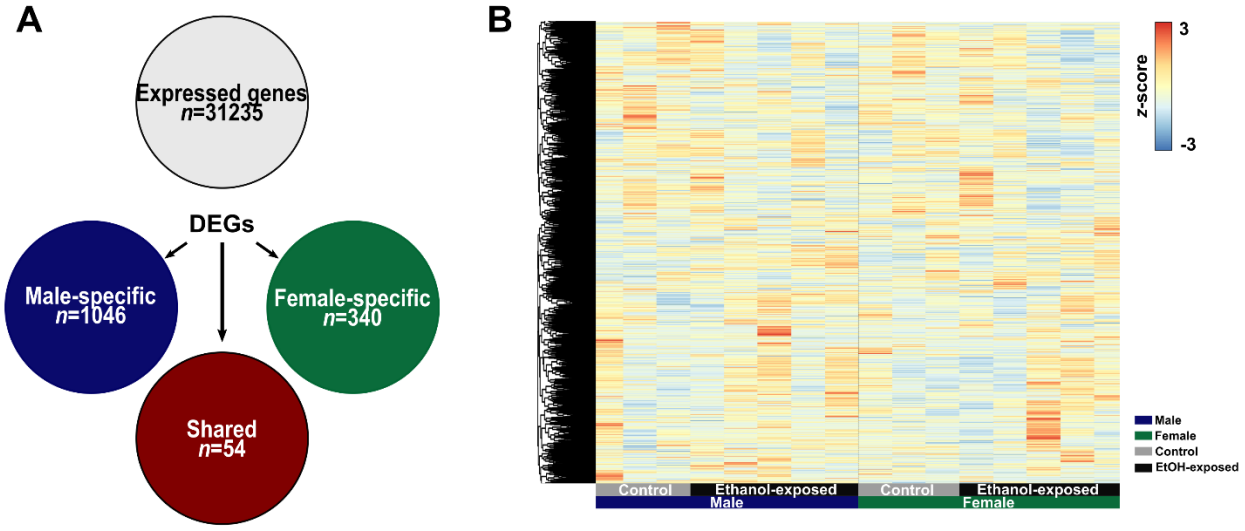


**Supplemental Figure 6: Establishing gene expression profiles in alcohol-exposed E18.5 placentas**

**A)** Schematic of sex-related differential transcriptomic analyses in male (Ctrl, *n*=3; EtOH, *n*=5) and female (Ctrl, *n*=3; EtOH, *n*=5) placentas at E18.5. Identification of all expressed genes in both sexes (*n*=31,235) and male-specific (*n*=1046), female-specific (*n*=340), and shared (*n*=54) DEGs. **B)** Heatmap of the gene expression levels (*z*-scores) of all analyzed genes (*n*=31,235) in individual male and female control and ethanol-exposed placentas. No clustering has been applied.

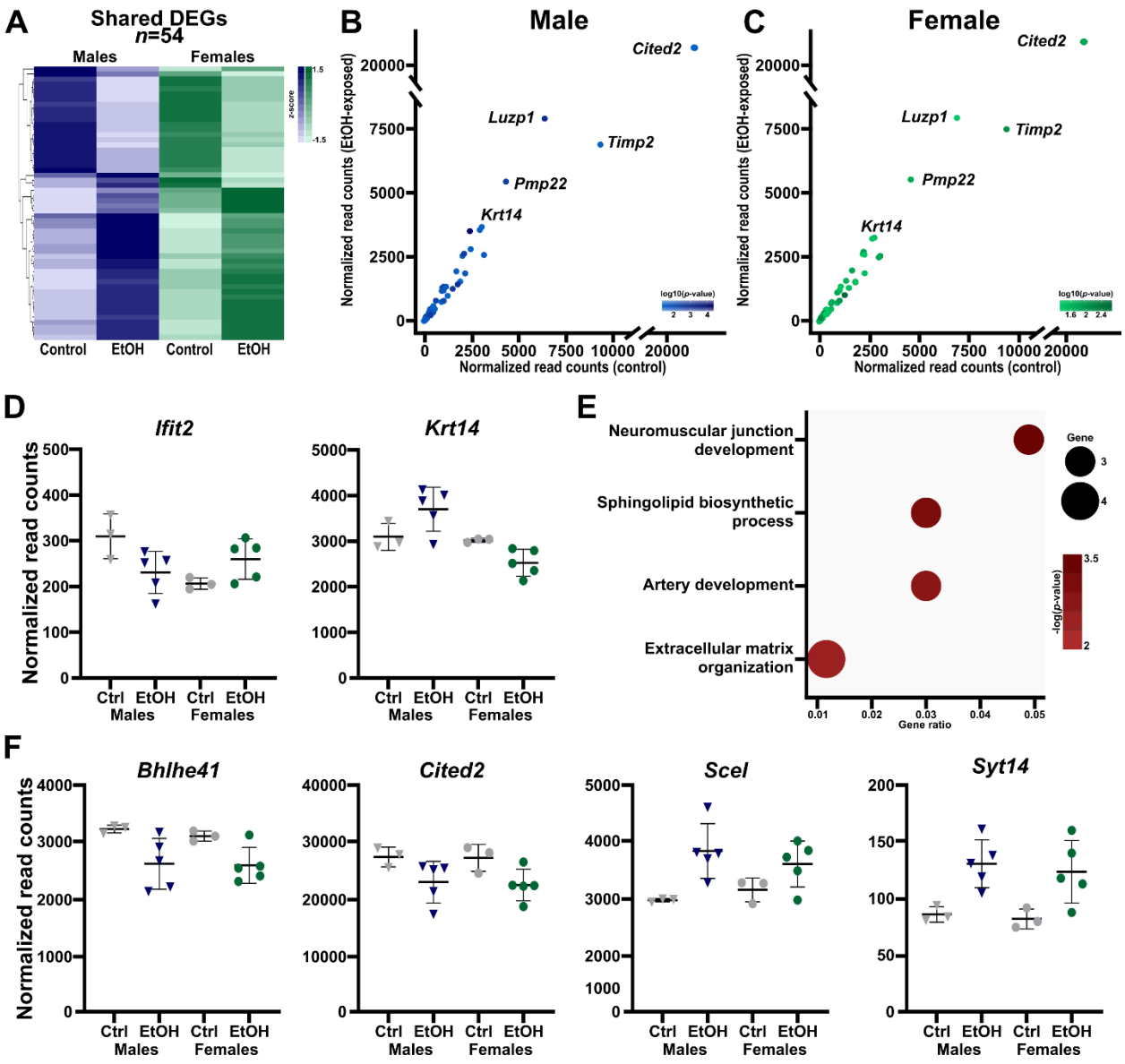


**Supplemental Figure 7: Shared DEGs are similarly altered in male and female ethanol-exposed placentas**

**A)** Heatmaps showing expression level (*z*-score) of common differentially expressed genes (DEGs) between male (blue; left) and female (green; right) placentas (*n*=54) following ethanol exposure. **B-C)** Scatterplots of the normalized read counts of the 54 common DEGs in **B)** male (blue; left) and **C)** female (green; right) control and ethanol-exposed placentas. **D)** Normalized read counts of 2/4 genes with opposing expression changes between male and female ethanol-exposed placentas. **E)** Top pathways

enriched for common DEGs (*n*=54) based on Metascape analysis. **F)** Normalized read counts of genes with altered expression in male and female ethanol-exposed placentas. Data represent the mean ± SD.

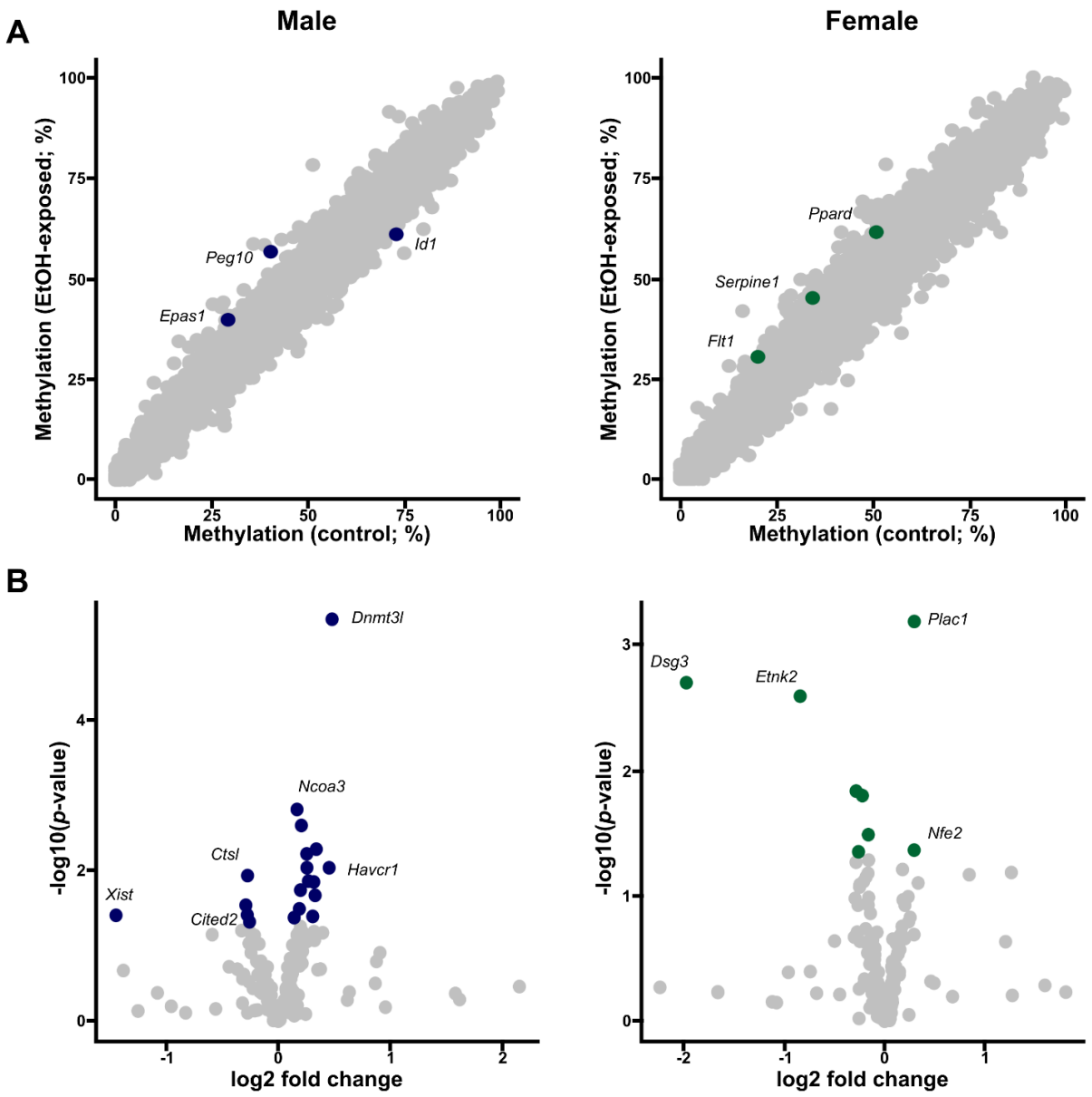


**Supplemental Figure 8: Early preimplantation alcohol exposure selectively alters the epigenetic profiles of placental development genes**

**A)** Scatterplot of the tiles located in placental development genes in control and ethanol-exposed male (left) and female (right) placentas. Blue (male) and green (female) dots represent tiles with ≥ 10% methylation changes in ethanol-exposed placentas compared to controls (males, $n$=3; females, $n$=3). **B)** Differential expression analyses of placental development genes between control and ethanol-exposed male (left) and female (right) placentas. Blue (male) and green (female) dots represent genes that were

significantly changed ($p<0.05$) in ethanol-exposed placentas (males $n=19$; females $n=8$) compared to controls.

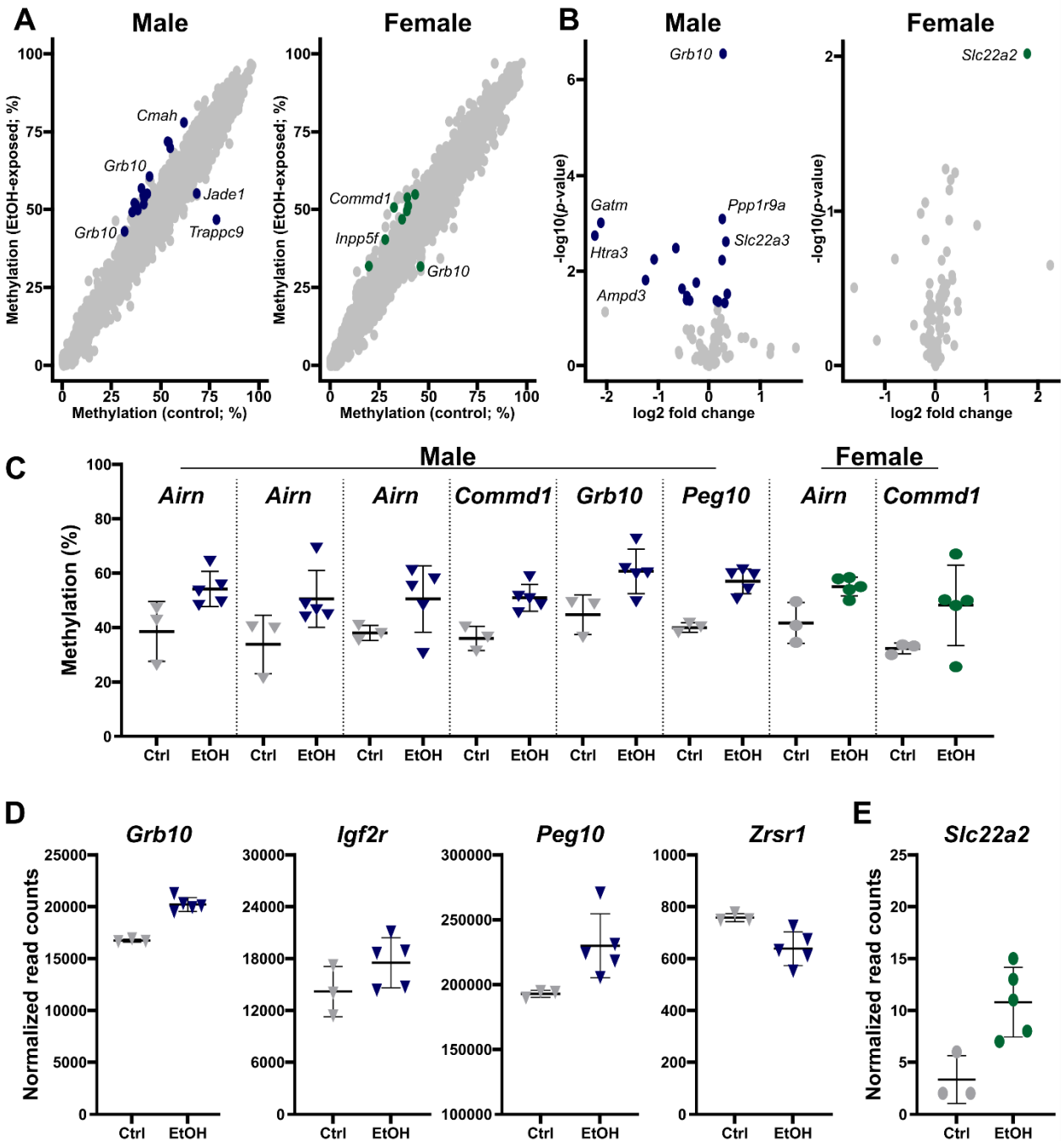


**Supplemental Figure 9: Early preimplantation alcohol exposure alters epigenetic profiles of placental imprinting genes in late-gestation placentas**

**A)** Scatterplot of tiles located in placental imprinting genes in control and ethanol-exposed male (left) and female (right) placentas. Blue (male) and green (female) dots represent tiles with ≥ 10% methylation changes in ethanol-exposed placentas (males, $n$=17; females, $n$=8) compared to controls. **B)** Differential

expression analysis of placental imprinting genes between control and ethanol-exposed male (left) and female (right) placentas. Blue (male) and green (female) dots represent genes that were significantly changed ($p<0.05$) in ethanol-exposed placentas (males, $n=18$; females, $n=1$) compared to controls. **C)** CpG methylation levels in control and ethanol-exposed male (left; grey/blue) and female (right; grey/green) placentas for DMRs located in placental imprinting genes. **D-E)** Normalized read counts of placental imprinting genes with altered expression in **D)** male (blue) and **E)** female (green) ethanol-exposed placentas compared to controls. Data are the mean ± SD.

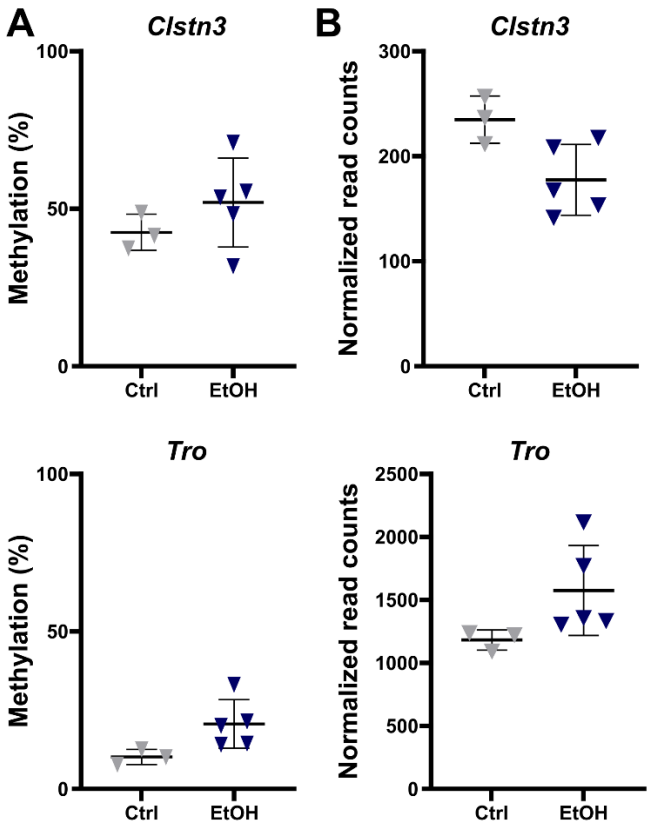


**Supplemental Figure 10: Growth-related genes with altered DNA methylation after ethanol exposure only show expression changes in male placentas**

**A)** CpG methylation levels in control and ethanol-exposed male placentas for DMRs located in the DEGs *Clstn3* (top) and *Tro* (bottom; *n*=3–5 for each group). **B)** Normalized read counts of *Clsnt3* (top) and *Tro* (bottom) in control and ethanol-exposed male placentas (*n*=3–5 for each group). All data represent the mean ± SD.

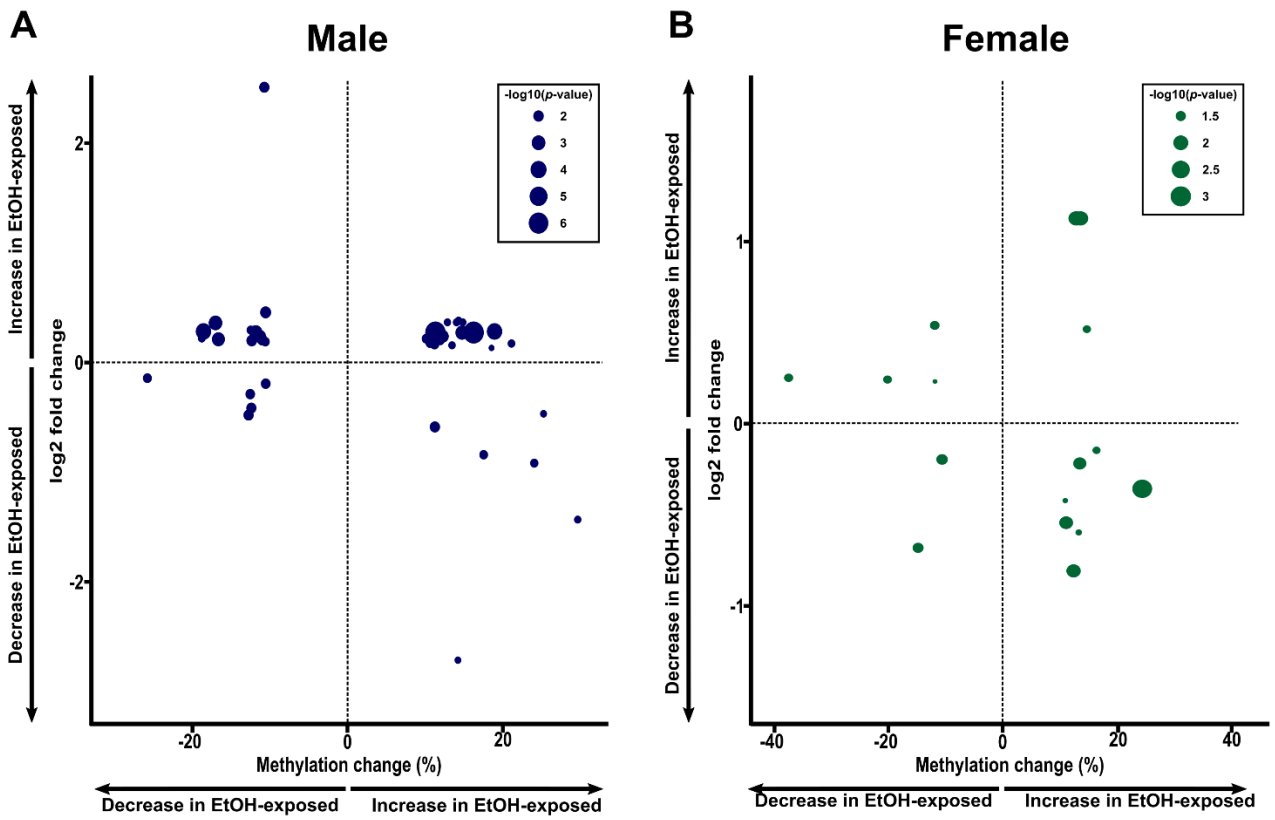


**Supplemental Figure 11: Differential expression is not directly linked to differential DNA methylation in late-gestation placentas following early preimplantation alcohol exposure**

**A-B)** DNA methylation differences between control and ethanol-exposed (X-axis) placentas and changes in gene expression (log2 fold change; Y-axis) in regions containing both DMRs and DEGs between control and ethanol-exposed placentas in **A)** males and **B)** females.

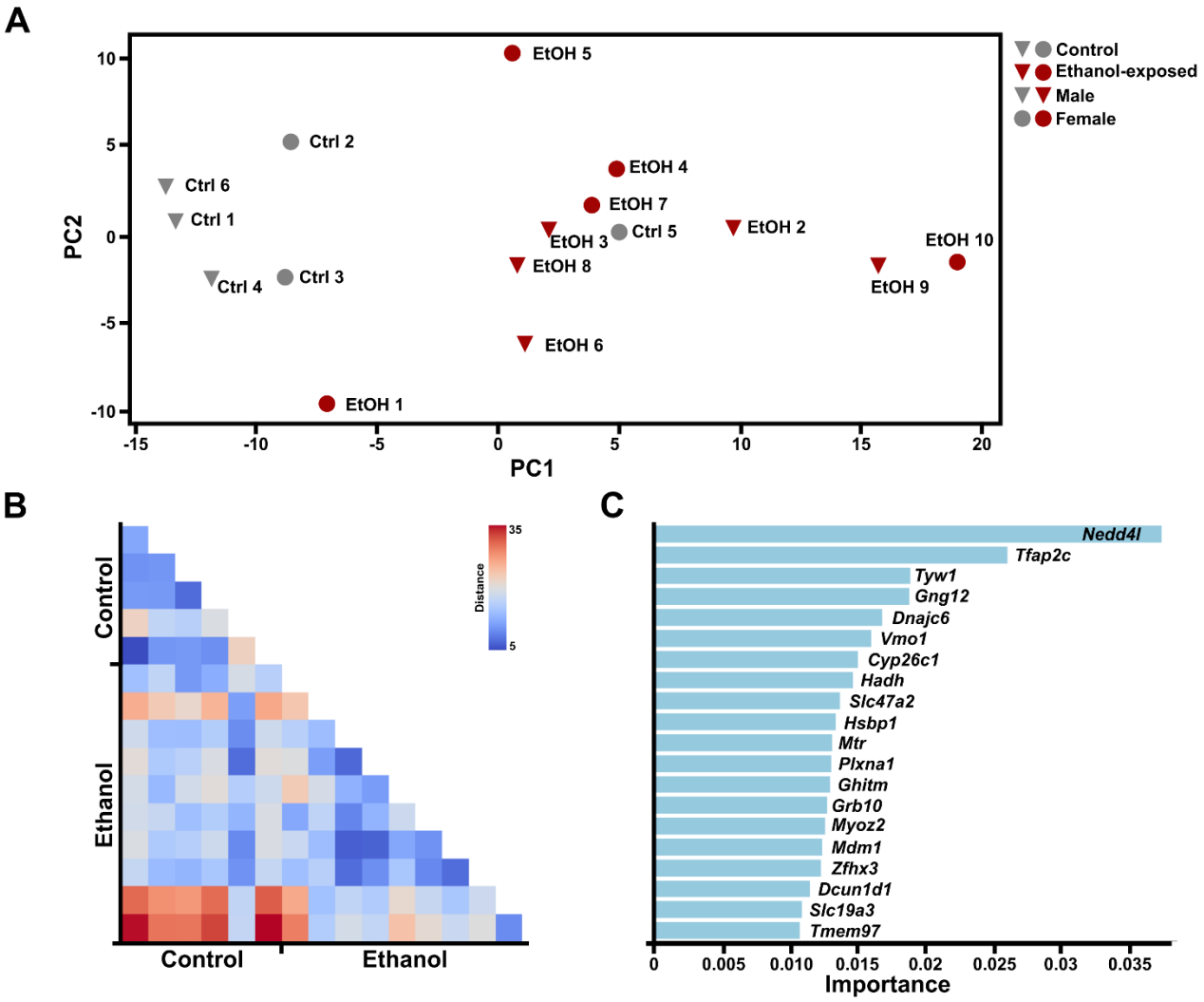


**Supplemental Figure 12: The transcriptomic signature of PAE does not enable PAE detection**

**A)** Principal component analysis showing the clustering of control and ethanol-exposed samples based on their CpG methylation levels in the 20 DEGs identified as possible transcriptomic biomarkers. **B)** Heatmap of the Euclidean distances of each control and ethanol-exposed sample based on their CpG methylation levels in the 20 potential biomarkers. **C)** Feature importance plot of the potential biomarkers based on LASSO analysis.

**SUPPLEMENTARY TABLES**

**Table S1: Male- and female-specific DMRs located in imprinting genes**

| Male-specific DMRs in imprinting genes | | | | | |
|---|---|---|---|---|---|
| **Effect of EtOH exposure** | **Gene symbol** | **Tile ID** | **Methylation change (%)** | **Annotation** | **In ICR?** |
| Decreased | *Trappc9* | chr15.72945601.72945700 | -31.79 | Intron | No |
| Decreased | *Phf17* | chr3.41556301.41556400 | -13.38 | Intron | No |
| Increased | *Peg13* | chr15.72810001.72810100 | 10.24 | Non-coding | Yes |
| Increased | *Grb10* | chr11.12025901.12026000 | 11.29 | Intron | Yes |
| Increased | *Peg13* | chr15.72809901.72810000 | 11.39 | Non-coding | Yes |
| Increased | *H13* | chr2.152670801.152670900 | 11.83 | Intron | No |
| Increased | *Airn* | chr17.12741901.12742000 | 11.94 | Intron | Yes |
| Increased | *Kcnq1ot1* | chr7.143295601.143295700 | 13.34 | Non-coding | Yes |
| Increased | *Airn* | chr17.12741801.12741900 | 13.60 | Intron | Yes |
| Increased | *Airn* | chr17.12741701.12741800 | 14.11 | Intron | Yes |
| Increased | *Nap1l5* | chr6.58906901.58907000 | 14.84 | Exon | Yes |
| Increased | *Commd1* | chr11.22973201.22973300 | 15.38 | Promoter-TSS | Yes |
| Increased | *Cmah* | chr13.24468301.24468400 | 15.96 | Intron | No |
| Increased | *Grb10* | chr11.12035301.12035400 | 16.20 | Intron | No |
| Increased | *Peg10* | chr6.4748601.4748700 | 16.47 | Intron | Yes |

| | | | | | |
|---|---|---|---|---|---|
| Increased | *Nap1l5* | chr6.58907001.58907100 | 17.25 | Promoter-TSS | Yes |
| Increased | *Nap1l5* | chr6.58907101.58907200 | 18.13 | Promoter-TSS | Yes |
| **Female-specific DMRs in imprinting genes** | | | | | |
| **Effect of EtOH exposure** | **Gene Name** | **Tile ID** | **Methylation change (%)** | **Annotation** | **In ICR?** |
| Decreased | *Grb10* | chr11.12025501.12025600 | -13.78 | Intron | Yes |
| Increased | *Art5* | chr7.102095201.102095300 | 10.68 | Non-coding | No |
| Increased | *Plagl1* | chr10.13090701.13090800 | 10.95 | Promoter-TSS | Yes |
| Increased | *H13* | chr2.152670901.152671000 | 11.87 | Intron | No |
| Increased | *Airn* | chr17.12742201.12742300 | 12.03 | Intron | Yes |
| Increased | *Pde10a* | chr17.8909701.8909800 | 12.48 | Intron | No |
| Increased | *Inpp5f* | chr7.128690801.128690900 | 12.72 | Intron | No |
| Increased | *Peg3* | chr7.6729401.6729500 | 14.97 | Intron | Yes |
| Increased | *Commd1* | chr11.22973101.22973200 | 18.60 | Promoter-TSS | Yes |

**Table S2: Male- and female-specific DEGs located in imprinting genes**

| Male-specific DEGs in imprinting genes | | | |
|---|---|---|---|
| **Effect of EtOH exposure** | **Gene Name** | **Log2FoldChange** | ***p*-value** |
| Decreased | *Htra3* | -2.220 | 0.002 |
| Decreased | *Gatm* | -2.103 | 0.001 |
| Decreased | *Ampd3* | -1.234 | 0.016 |
| Decreased | *Dcn* | -1.068 | 0.006 |
| Decreased | *Qpct* | -0.645 | 0.003 |
| Decreased | *Rasgrf1* | -0.525 | 0.024 |
| Decreased | *Ano1* | -0.437 | 0.041 |
| Decreased | *Tnfrsf23* | -0.430 | 0.034 |
| Decreased | *Osbpl5* | -0.377 | 0.042 |
| Decreased | *Zrsr1* | -0.248 | 0.018 |
| Increased | *Gab1* | 0.142 | 0.042 |
| Increased | *Ube3a* | 0.183 | 0.045 |
| Increased | *Peg10* | 0.254 | 0.006 |
| Increased | *Ppp1r9a* | 0.258 | 0.001 |
| Increased | *Grb10* | 0.273 | <0.001 |
| Increased | *Igf2r* | 0.307 | 0.048 |
| Increased | *Slc22a3* | 0.327 | 0.002 |
| Increased | *Cobl* | 0.354 | 0.031 |

| Female-specific DEGs in imprinting genes | | | |
|---|---|---|---|
| **Effect of EtOH exposure** | **Gene Name** | **Log2FoldChange** | ***p*-value** |
| Increased | *Slc22a2* | 1.792 | 0.010 |